Mathematisches Forschungsinstitut Oberwolfach

Report No. 16/2021

DOI: 10.4171/OWR/2021/16

Small Collaboration: Numerical Analysis of Electromagnetic Problems (hybrid meeting)

Organized by
Fleurianne Bertrand, Twente
Matthias Schlottbom, Twente
Gerhard Starke, Essen

21 March – 27 March 2021

Abstract. The classical theory of electromagnetism describes the interaction of electrically charged particles through electromagnetic forces, which are carried by the electric and magnetic fields. The propagation of the electromagnetic fields can be described by Maxwell's equations. Solving Maxwell's equations numerically is a challenging problem which appears in many different technical applications. Difficulties arise for instance from material interfaces or if the geometrical features are much larger than or much smaller than a typical wavelength. The spatial discretization needs to combine good geometrical flexibility with a relatively high order of accuracy. The aim of this small-scale, week-long interactive mini-workshop jointly organized by the University of Duisburg-Essen and the University of Twente, and kindly hosted at the MFO, is to bring together experts in non-standard and mixed finite elements methods with experts in the field of electromagnetism.

Mathematics Subject Classification (2010): 65N12, 65N30.

Introduction by the Organizers

This small-scale workshop continued the tradition of fruitful interactions between applied mathematics and computational engineering focusing on computational electromagnetism. A focal point of the workshop was the deep understanding of Maxwell's equations leading to efficient and robust simulation methods in computational electromagnetics. Several mathematical and numerical aspects of emerging methodologies in mixed finite element methods and their applications in computational electromagnetism were covered.

In particular, the general framework of variationally consistent discretization schemes for obstacle-type problems benefited from this intense personal interaction. In this framework, the constraints are weakly incorporated and lead to a saddle-point problem. Since the Lagrange multiplier represents the surface forces such methods play a crucial role in many applications. Optimal convergence rates can be established using a uniform inf-sup bound, but complementarity terms have to be taken into account, leading to a non-linear and non-differentiable formulation.

The low regularity of the solution requires tailored discretizations together with a careful analysis. Inspiring talks reviewing open problems in this field were given, which resulted in deep discussionss about Discontinuous Galerkin methods for Maxwell's equations.

Further research directions were explored, ranging from frameworks for structure-preserving discretizations to algorithms for stochastic partial differential equations that are able to overcome the curse of dimensionality. A distinguished lecture enlightened us towards new approaches for stochastic partial differential equations in electromagnetism.

In addition to these keynote lectures, fourteen talks fostered fruitful discussions between mathematicians of the University of Twente and the University of Duisburg-Essen and laid the groundwork for future collaborations. The remainder of this report contains the extended abstracts and illustrates the wide range of research areas tackled during this workshop.

Small Collaboration (hybrid meeting): Numerical Analysis of Electromagnetic Problems

Table of Contents

Abstracts

Obstacle Problems in Electromagnetic Shielding & Numerical Analysis for Maxwell Obstacle Problems

Irwin Yousept, Maurice Hensel

Electromagnetic (EM) shielding is a physical process of canceling or redirecting EM waves in a certain domain of interest by means of obstacles made of conducting or magnetic materials. It was first discovered by Michael Faraday in 1836, who experimentally verified that a conductive enclosure (Faraday cage) is able to eliminate the effect of an external electric field by charge cancelation on the boundary and leaving zero field inside the cage. On the other hand, a specific magnetic material can realize shielding by diverting the external magnetic flux to another direction. Typical materials used in Faraday shielding are conductive sheet metals and metallic alloys, whereas ferromagnetic materials are widely used for magnetic obstacles. Today, EM shielding is indispensable not only for high-technological applications but also for many of our daily used electronic devices.

From the mathematical point of view, EM shielding falls into the class of obstacle problems (cf. Duvaut and Lions [1]). More precisely, in the free region, the EM waves satisfy the fundamental Maxwell equations, whereas in the shielded area obstacle constraints are applied to the fields. To formulate the corresponding mathematical formulation, let us denote by $\Omega \subset \mathbb{R}^3$ an open set (not necessarily connected, Lipschitz, or bounded) representing the domain of interest and set

$$\boldsymbol{H}(\mathbf{curl}) := \big\{ \boldsymbol{q} \in \boldsymbol{L}^2(\Omega) \;\big|\; \mathbf{curl}\, \boldsymbol{q} \in \boldsymbol{L}^2(\Omega) \big\}, \quad \boldsymbol{H}_0(\mathbf{curl}) := \overline{\boldsymbol{\mathcal{C}}_0^\infty(\Omega)}^{\|\cdot\|_{\boldsymbol{H}(\mathbf{curl})}}.$$

Furthermore, let $\mathbf{0} \in \boldsymbol{K} \subset \boldsymbol{L}^2(\Omega) \times \boldsymbol{L}^2(\Omega)$ be a closed and convex subset standing for the underlying feasible (constraint) set. Then, given initial data $(\boldsymbol{E}_0, \boldsymbol{H}_0) \in \{\boldsymbol{H}_0(\mathbf{curl}) \times \boldsymbol{H}(\mathbf{curl})\} \cap \boldsymbol{K}$ and an applied current source $\boldsymbol{f} \in \mathcal{C}^{0,1}((0,T), \boldsymbol{L}^2(\Omega))$, we look for $(\boldsymbol{E}, \boldsymbol{H}) \in W^{1,\infty}((0,T), \boldsymbol{L}^2(\Omega) \times \boldsymbol{L}^2(\Omega))$ s.t.

$$(1) \quad \begin{cases} \displaystyle\int_0^T \int_\Omega \epsilon \partial_t \boldsymbol{E} \cdot (\boldsymbol{v} - \boldsymbol{E}) + \mu \partial_t \boldsymbol{H} \cdot (\boldsymbol{w} - \boldsymbol{H}) - \boldsymbol{H} \cdot \mathbf{curl}\, \boldsymbol{v} + \boldsymbol{E} \cdot \mathbf{curl}\, \boldsymbol{w} \\ \displaystyle\geq \int_0^T \int_\Omega \boldsymbol{f} \cdot (\boldsymbol{v} - \boldsymbol{E}) \\ \forall (\boldsymbol{v}, \boldsymbol{w}) \in L^2((0,T), \boldsymbol{H}_0(\mathbf{curl}) \times \boldsymbol{H}(\mathbf{curl})),\ (\boldsymbol{v}, \boldsymbol{w})(t) \in \boldsymbol{K} \text{ a.e. } t \in (0,T) \\ (\boldsymbol{E}, \boldsymbol{H})(t) \in \boldsymbol{K} \text{ for all } t \in [0,T] \\ (\boldsymbol{E}, \boldsymbol{H})(0) = (\boldsymbol{E}_0, \boldsymbol{H}_0). \end{cases}$$

Here, the electric permittivity and the magnetic permeability $\epsilon, \mu : \Omega \to \mathbb{R}^{3\times 3}$ are assumed to be of class $L^\infty(\Omega)^{3\times 3}$, symmetric, and uniformly positive definite in the sense that there exist positive constants $\underline{\epsilon}, \underline{\mu} > 0$ such that

$$\xi^T \epsilon(x) \xi \geq \underline{\epsilon} |\xi|^2 \quad \text{and} \quad \xi^T \mu(x) \xi \geq \underline{\mu} |\xi|^2 \quad \text{for a.e. } x \in \Omega \text{ and all } \xi \in \mathbb{R}^3.$$

In [3, Theorem 1], the author proved an existence result for (1) built on [2, Theorem 3.11]. The developed result yields only existence in $W^{1,\infty}((0,T), \boldsymbol{L}^2(\Omega) \times \boldsymbol{L}^2(\Omega))$ without the global **curl** regularity, i.e., $(\boldsymbol{E}, \boldsymbol{H}) \in L^2((0,T), \boldsymbol{H}_0(\mathbf{curl}) \times \boldsymbol{H}(\mathbf{curl}))$ is not guaranteed. Nonetheless, the solution is still physically reasonable as it turns to obey the physical electromagnetic laws in the free regions. More precisely, if we denote the electric (resp. magnetic) free region by the open (possibly empty) subset $\Omega_E \subset \Omega$ (resp. $\Omega_H \subset \Omega$), i.e., if

$$(\boldsymbol{v}, \boldsymbol{w}) \in \boldsymbol{K} \Rightarrow (\tilde{\boldsymbol{v}}, \tilde{\boldsymbol{w}}) \in \boldsymbol{K} \quad \forall \tilde{\boldsymbol{v}} = \begin{cases} \boldsymbol{v}_E & \text{in } \Omega_E \\ \boldsymbol{v} & \text{elsewhere} \end{cases} \qquad \tilde{\boldsymbol{w}} = \begin{cases} \boldsymbol{w}_H & \text{in } \Omega_H \\ \boldsymbol{w} & \text{elsewhere} \end{cases}$$

holds for any $(\boldsymbol{v}_E, \boldsymbol{w}_H) \in \boldsymbol{L}^2(\Omega_E) \times \boldsymbol{L}^2(\Omega_H)$, then every solution $(\boldsymbol{E}, \boldsymbol{H}) \in W^{1,\infty}((0,T), \boldsymbol{L}^2(\Omega) \times \boldsymbol{L}^2(\Omega))$ of (1) fulfils the Maxwell-Ampère equation in Ω_E and the Faraday law in Ω_H:

$$\text{(2)} \qquad \begin{cases} \epsilon \partial_t \boldsymbol{E} - \mathbf{curl}\, \boldsymbol{H} = \boldsymbol{f} & \text{a.e. in } \Omega_E \times (0,T) \\ \mu \partial_t \boldsymbol{H} + \mathbf{curl}\, \boldsymbol{E} = \boldsymbol{0} & \text{a.e. in } \Omega_H \times (0,T). \end{cases}$$

In particular, every solution to (1) enjoys the local regularity properties

$$\mathbf{curl}\, \boldsymbol{E} \in L^\infty((0,T), \boldsymbol{L}^2(\Omega_H)) \quad \text{and} \quad \mathbf{curl}\, \boldsymbol{H} \in L^\infty((0,T), \boldsymbol{L}^2(\Omega_E)),$$

and if $\Omega_H = \Omega$ then the electric boundary condition is fully recovered, i.e., $\boldsymbol{E} \in L^\infty((0,T), \boldsymbol{H}_0(\mathbf{curl}))$. All these results were proven in [3, Theorem 1].

The uniqueness analysis of (1) turns out to be more challenging and requires a careful treatment. We notice that energy arguments are not applicable due to the poor regularity of the solution. Under a structural assumption on the feasible set $\boldsymbol{K}$ (see [3, Assumption 1.1]), the author established a uniqueness result [3, Theorem 2]. The proof is based on a local $\boldsymbol{H}(\mathbf{curl})$-regularity analysis with respect to the constraint set under Assumption 1.1, in particular under a separation ansatz between the electric and magnetic obstacle sets. As shown there, the uniqueness holds also true if $\Omega_H = \Omega$ (pure electric obstacle problem) or $\Omega_E = \Omega$ (pure magnetic obstacle problem). As a consequence of Theorems 1 and 2 in [3], for any given closed and convex feasible electric set $\boldsymbol{0} \in \boldsymbol{K}_E \in \boldsymbol{L}^2(\Omega)$, the pure electric obstacle problem

$$\text{(PE)} \qquad \begin{cases} \displaystyle\int_\Omega \epsilon \partial_t \boldsymbol{E}(t) \cdot (\boldsymbol{v} - \boldsymbol{E}(t)) - \boldsymbol{H}(t) \cdot \mathbf{curl}(\boldsymbol{v} - \boldsymbol{E}(t)) \geq \int_\Omega \boldsymbol{f}(t) \cdot (\boldsymbol{v} - \boldsymbol{E}(t)) \\ \text{for all } \boldsymbol{v} \in \boldsymbol{H}_0(\mathbf{curl}) \cap \boldsymbol{K}_E \text{ and a.e. } t \in (0,T) \\ \mu \partial_t \boldsymbol{H}(t) + \mathbf{curl}\, \boldsymbol{E}(t) = \boldsymbol{0} \text{ for a.e. } t \in (0,T) \\ \boldsymbol{E}(t) \in \boldsymbol{K}_E \text{ for all } t \in [0,T] \\ (\boldsymbol{E}, \boldsymbol{H})(0) = (\boldsymbol{E}_0, \boldsymbol{H}_0) \end{cases}$$

admits a unique solution

$$(\boldsymbol{E}, \boldsymbol{H}) \in L^\infty((0,T), \boldsymbol{H}_0(\mathbf{curl}) \times \boldsymbol{L}^2(\Omega)) \cap W^{1,\infty}((0,T), \boldsymbol{L}^2(\Omega) \times \boldsymbol{L}^2(\Omega)).$$

We note that (PE) preserves the Faraday law but modifies the Maxwell-Ampère equation $\epsilon\partial_t \boldsymbol{E} - \mathbf{curl}\, \boldsymbol{H} = \boldsymbol{f}$ into a variational inequality of the first kind. Similarly, for any given closed and convex feasible magnetic set $\mathbf{0} \in \boldsymbol{K}_H \in \boldsymbol{L}^2(\Omega)$, the pure magnetic obstacle problem

$$\text{(PH)} \qquad \begin{cases} \displaystyle\int_\Omega \mu\partial_t \boldsymbol{H}(t)\cdot(\boldsymbol{w}-\boldsymbol{H}(t)) + \boldsymbol{E}(t)\cdot\mathbf{curl}(\boldsymbol{w}-\boldsymbol{H}(t)) \geq 0 \\ \text{for all } \boldsymbol{w} \in \boldsymbol{H}(\mathbf{curl}) \cap \boldsymbol{K}_H \text{ and a.e. } t \in (0,T) \\ \epsilon\partial_t \boldsymbol{E}(t) - \mathbf{curl}\, \boldsymbol{H}(t) = \boldsymbol{f}(t) \text{ for a.e. } t \in (0,T) \\ \boldsymbol{H}(t) \in \boldsymbol{K}_H \text{ for all } t \in [0,T] \\ (\boldsymbol{E},\boldsymbol{H})(0) = (\boldsymbol{E}_0,\boldsymbol{H}_0) \end{cases}$$

admits a unique solution

$$(\boldsymbol{E},\boldsymbol{H}) \in L^\infty((0,T),\boldsymbol{L}^2(\Omega)\times\boldsymbol{H}(\mathbf{curl}))\cap W^{1,\infty}((0,T),\boldsymbol{L}^2(\Omega)\times\boldsymbol{L}^2(\Omega)).$$

Differently from (PE), the magnetic shielding case (PH) preserves the Maxwell-Ampère equation and modifies the Faraday law by a variational inequality of the first kind. The well-posedness results for (1), (PE), and (PH) serve as a basis for further investigations, including

- finite element analysis
- ferromagnetic shielding
- shape optimal design

which have been the subject of our ongoing research. The Eddy Current approximation of (PE) is investigated in [6].

Let us next discuss the finite element analysis of (PE) for

$$\boldsymbol{K}_E = \{\boldsymbol{v} \in \boldsymbol{L}^2(\Omega) \;\big|\; |\boldsymbol{v}(x)| \leq d \text{ for a.e. } x \in \omega\}$$

and scalar-valued material parameters. Here, we rely on $\Omega \subset \mathbb{R}^3$ and $\omega \subset\subset \Omega$ to be bounded and polyhedral Lipschitz domains. Denote by $\{\mathcal{T}_h\}_{h>0}$ a quasi-uniform family of triangulations, s.t.

$$\overline{\Omega} = \bigcup_{T\in\mathcal{T}_h} T, \quad \overline{\omega} = \bigcup_{T\in\mathcal{T}_h^\omega} T,$$

with $\epsilon_{|T}, \mu_{|T}$ and $\sigma_{|T}$ being constant for all $T \in \mathcal{T}_h$. To obtain a fully discrete scheme we use a mixed FEM in space. Based on this triangulation, we use the well-known finite element spaces

$$\mathbf{ND}_h^0 = \{\boldsymbol{v}_h \in \boldsymbol{H}_0(\mathbf{curl}) \mid \boldsymbol{v}_{h|_T} = a_T + b_T \times \cdot \text{ for some } a_T, b_T \in \mathbb{R}^3 \;\forall T \in \mathcal{T}_h\},$$
$$\mathbf{DG}_h = \{\boldsymbol{w}_h \in \boldsymbol{L}^2(\Omega) \mid \boldsymbol{w}_{h|_T} = a_T \text{ for some } a_T \in \mathbb{R}^3 \;\forall T \in \mathcal{T}_h\}.$$

We are interested in comparing two different discretizations in time. Starting with the implicit Euler scheme, let us consider the canonical partition

$$\tau = \frac{T}{N}, \quad t_n = n\tau \quad \forall n \in \{0,\dots,N\}, \quad N \in \mathbb{N}.$$

Using Nédélec's elements for the electric field $\boldsymbol{E}$ and piecewise constant elements for the magnetic field $\boldsymbol{H}$ we invoke a standard decoupling to derive the following fully discrete scheme:

$$\begin{cases} \text{Find } \{(\boldsymbol{E}_h^n, \boldsymbol{H}_h^n)\}_{n=1}^N \subset \left(\boldsymbol{K}_E \cap \mathbf{ND}_h^0\right) \times \mathbf{DG}_h, \text{ s.t.} \\ \displaystyle\int_\Omega \epsilon \boldsymbol{E}_h^n \cdot (\boldsymbol{v}_h - \boldsymbol{E}_h^n) + \tau^2 \mu^{-1} \operatorname{\mathbf{curl}} \boldsymbol{E}_h^n \cdot \operatorname{\mathbf{curl}}(\boldsymbol{v}_h - \boldsymbol{E}_h^n) \\ \displaystyle\geq \int_\Omega (\tau \boldsymbol{f}^n + \boldsymbol{E}_h^{n-1}) \cdot (\boldsymbol{v}_h - \boldsymbol{E}_h^n) + \tau \boldsymbol{H}_h^{n-1} \cdot \operatorname{\mathbf{curl}}(\boldsymbol{v}_h - \boldsymbol{E}_h^n) \quad \forall \boldsymbol{v}_h \in \boldsymbol{K}_E \cap \mathbf{ND}_h \\ \boldsymbol{H}_h^n = \boldsymbol{H}_h^{n-1} - \tau \mu^{-1} \operatorname{\mathbf{curl}} \boldsymbol{E}_h^n. \end{cases}$$

The left-hand side of the variational inequality induces a coercive and bounded bilinear form, as a result of which the well-posedness of the system follows from a standard result by Lions & Stampacchia. Note that the above VI features a **curl curl**-structure. Additionally, at every step, a non-smooth solver is required to approximate its solution. This makes the numerical realization of this scheme very demanding in terms of computational cost, especially when considering fine discretizations in time. To overcome the need for a non-smooth solver, we propose a different time discretization: Motivated by the work of Yee in 1966 (cf. [4]), we consider the Amperé-Maxwell VI in (PE) at the intermediate time steps $t_{n-\frac{1}{2}} = t_n - \frac{\tau}{2}$ and the Faraday equation in (PE) at the time steps t_n. In contrast to the previous mixed FEM, we now use Nédélec's elements for the magnetic field $\boldsymbol{H}$ and piecewise constant elements for the electric field $\boldsymbol{E}$. Approximating time derivatives by central differences, we obtain the following fully discrete scheme:

$$\begin{cases} \text{Find } \{(\boldsymbol{E}_h^{n-\frac{1}{2}}, \boldsymbol{H}_h^{n+\frac{1}{2}})\}_{n=1}^N \subset (\boldsymbol{K}_E \cap \mathbf{DG}_h) \times \mathbf{ND}_h, \text{ s.t.} \\ \displaystyle\int_\Omega \epsilon \delta \boldsymbol{E}_h^n \cdot (\boldsymbol{v}_h - \boldsymbol{E}_h^{n-\frac{1}{2}}) - \operatorname{\mathbf{curl}} \boldsymbol{H}_h^{n-\frac{1}{2}} \cdot (\boldsymbol{v}_h - \boldsymbol{E}_h^{n-\frac{1}{2}}) \\ \displaystyle\geq \int_\Omega \boldsymbol{f}_h^{n-\frac{1}{2}} \cdot (\boldsymbol{v}_h - \boldsymbol{E}_h^{n-\frac{1}{2}}) \quad \forall \boldsymbol{v}_h \in \boldsymbol{K}_E \cap \mathbf{DG}_h \quad \forall n \in \{1, \dots, N\} \\ \boldsymbol{E}_h^n = 2\boldsymbol{E}_h^{n-\frac{1}{2}} - \boldsymbol{E}_h^{n-1} \\ \displaystyle\int_\Omega \mu \delta \boldsymbol{H}_h^{n+\frac{1}{2}} \cdot \boldsymbol{w}_h + \boldsymbol{E}_h^n \cdot \operatorname{\mathbf{curl}} \boldsymbol{w}_h = \mathbf{0} \quad \forall \boldsymbol{w}_h \in \mathbf{ND}_h \quad \forall n \in \{1, \dots, N\}. \end{cases}$$

Note that the obstacle is now discretized at $t_{n-\frac{1}{2}}$ rather than at t_n and that the VI admits an $\boldsymbol{L}^2$-structure. Thus, the solution is given by a projection formula which can explicitly be stated in terms of the data. This results in the fact that, at every step, the main effort consists of solving the linear Faraday equation, leading to very low computation times when compared to the implicit Euler. The convergence analysis for the (Yee-)scheme is mainly complicated due to the lack of global $\boldsymbol{L}^2$-regularity of $\operatorname{\mathbf{curl}} \boldsymbol{H}_h^{n-\frac{1}{2}}$. Heavily related to the property (2) of the solution to (1), the term $\operatorname{\mathbf{curl}} \boldsymbol{H}_h^{n-\frac{1}{2}}$ does not admit a uniform $\boldsymbol{L}^2$-bound in Ω - only in $\Omega \setminus \omega$. Inside the obstacle ω we are only able to show a weaker $\boldsymbol{L}^1$-bound. This fact is somehow justified by the mentioned low regularity issue in

(PE). Therefore, our first step consists of bypassing the missing boundedness by exploiting the standard quasi-interpolation operator onto $\mathbf{DG}_h$ for smooth and compactly supported fields. In this way, we are able to derive a convergence result towards a solution of a time integrated version of the variational inequality in (PE) involving fewer test functions $\boldsymbol{v} \in \boldsymbol{K}_E \cap \boldsymbol{\mathcal{C}}_0^\infty(\Omega)$. The final step of enlarging the test function set to $\boldsymbol{K}_E \cap \boldsymbol{H}_0(\mathbf{curl})$ requires us to construct a constraint preserving mollification operator in the spirit of Ern and Guermond (cf. [5]).

References

[1] G. Duvaut and J.-L. Lions, *Inequalities in mechanics and physics*, Springer-Verlag, Berlin-New York, 1976.

[2] I. Yousept, *Hyperbolic Maxwell variational inequalities of the second kind*, ESAIM: COCV 26 (2020), 34 (23pp).

[3] I. Yousept, *Well-posedness theory for electromagnetic obstacle problems*, Journal of Differential Equations 269 (2020), pp. 8855–8881.

[4] K. Yee, *Numerical solution of initial boundary value problems involving Maxwell's equations in isotropic media,* IEEE Transactions on Antennas and Propagation, 14(3):302–307, 1966.

[5] A. Ern and J.-L. Guermond, *Mollification in strongly Lipschitz domains with application to continuous and discrete de Rham complexes,* Comput. Methods Appl. Math., 16(1):51–75, 2016

[6] M. Hensel and I. Yousept, *Eddy Current Approximation in Maxwell Obstacle Problems,* Submitted, 2021

Resonance phenomena and construction of metamaterials

Agnes Lamacz-Keymling

(joint work with Patrizia Donato, Ben Schweizer)

Many modern key technologies are modeled through partial differential equations involving multiple small scales. Such equations are often hard to treat numerically, since the corresponding solutions are typically highly oscillatory and the microstructure has to be resolved to capture the main features of the underlying model. However under structural assumptions such as periodicity an effective large scale behavior is observed.

The mathematical analysis of the effective properties of multiscale models became possible with the development of the method of homogenization in the 1970s. The homogenization technique was successfully applied to a variety of equations ranging from porous media to Maxwell's equations. In the standard situation, the homogenization result is of the following form: Given an ε-periodic coefficient a^ε and a corresponding solution sequence u^ε, every weak limit u of u^ε satisfies the original equation with a constant effective coefficient a^{eff}. Even though the dependence of a^{eff} on the microstructure is already non-trivial, its computation is based on averaging. In particular such a standard homogenization result cannot lead to a qualitatively different equation for the limit u.

The analysis of metamaterials eludes this standard framework. Metamaterials are composites of ordinary materials arranged in small substructures. A smart choice of the microscopic geometry can lead to astonishing effective properties

of the medium that are not shared by any of its constituents. Typically such effects are obtained by micro-structures involving a high contrast in the parameters and/or singular geometries such as thin wires [1] or small perforations [2] whose volume fraction vanishes in the limit $\varepsilon \to 0$.

In this talk we discuss two results that are based on resonance. The first result focuses on the mathematical analysis of negative index metamaterials. An early study of the electrodynamics of media with negative refractive index, which are characterized through simultaneously negative values of the permittivity ε and the magnetic permeability μ, was first provided by Veselago [7]. Since no natural material exhibits a negative permeability μ, the result of Veselago remained purely theoretical until in 1999 first ideas have been published on the construction of an actual negative index metamaterial by using a periodic structure consisting of small highly conductive split-rings and wires, see e.g. [6].

Our aim is to explain the effective behavior of this construction in the framework of homogenization. To this end, in [4, 5] we study a scattering problem for the time harmonic Maxwell's equations in a complex geometry involving a small parameter $\eta > 0$ which characterizes the typical size of the microstructure,

$$\begin{aligned} \mathrm{curl} E^\eta &= i\omega H^\eta, \\ \mathrm{curl} H^\eta &= -i\omega \varepsilon_\eta E^\eta. \end{aligned}$$

The homogenization process is performed in the case that many (order η^{-3}) small (order η), flat (order η^2) and highly conductive (order η^{-3}) metallic split-rings are distributed in a scattering domain $\Omega \subset \mathbb{R}^3$. In addition the split-ring array is combined with thin (order η^2) highly conducting (order η^{-2}) metallic wires. It is important to highlight that the entire behavior of the microstructure is encoded in a single parameter, namely the η-dependent permittivity ε_η, which involves a high contrast as well as the complex geometry of the split-ring wire structure.

We determine the effective behavior of this metamaterial in the limit $\eta \to 0$. As a main feature we find that the effects of the rings and of the wires are effectively decoupled. Even though both original materials (metal and void) have the same positive magnetic permeability $\mu = 1$, the effective Maxwell system exhibits, depending on the frequency ω, a negative magnetic response. This effect is based on resonances in the small split-rings which together with a careful choice of the frequency and the geometry of the rings leads to a negative effective permeability μ^{eff}.

The wires operate in a less sophisticated way. On the one hand, due to their vanishing volume fraction, the wires do not affect the parameter μ^{eff}. On the other hand, due to their particular topology (in the limit $\eta \to 0$ they form connected lines), they influence the effective permittivity $\varepsilon^{\mathrm{eff}}$ through an averaging process. If the permittivity ε_η in the wires is negative, which is typically the case for metals, the effective permittivity $\varepsilon^{\mathrm{eff}}$ inherits this feature in the homogenization limit.

In the second setting, see [3], we analyze the Helmholtz equation

$$\begin{aligned} -\Delta u^\varepsilon - \omega^2 u^\varepsilon &= f \quad \text{in } \Omega_\varepsilon \\ \partial_n u^\varepsilon &= 0 \quad \text{on } \partial\Omega_\varepsilon \end{aligned}$$

in a complex domain Ω_ε, where a sound absorbing structure at one part of the boundary is modeled by a periodic geometry with periodicity $\varepsilon > 0$. A resonator volume of thickness ε is connected with thin channels (opening ε^3) of length ε with the main part of the macroscopic domain Ω_0. We ask for the effective influence of the small resonators to find that the weak limit u of u^ε is characterized through the same Helmholtz equation in the limit domain Ω_0. Hence the effect of the structure gets lost at leading order. A deeper insight can be gained by studying the first order corrector $w^\varepsilon := \frac{u^\varepsilon - u}{\varepsilon}$ and its weak limit w. It turns out that w satisfies an effective Helmholtz equation with a non-homogeneous Neumann boundary condition which is understood as a sound absorbing effect. The magnitude of the effect depends on the frequency ω of the system and can be very large for ω close to the resonant frequency.

References

[1] M. Bouchitté, D. Felbacq, *Homogenization of a wire photonic crystal: the case of small volume fraction*, SIAM J. Appl. Math **6** (2006), 2061–2084.

[2] D. Cioranescu, F. Murat, *A strange term coming from nowhere*, Topics in the mathematical modelling of composite materials. Birkhäuser Boston, Boston, MA (1997), 45–93.

[3] P. Donato, A. Lamacz, B. Schweizer, *Sound absorption by perforated walls along boundaries*, Applicable Analysis, published online https://doi.org/10.1080/00036811.2020.1855329 (2020).

[4] A. Lamacz, B. Schweizer, *Effective Maxwell equations in a geometry with flat rings of arbitrary shape*, SIAM J. Math. Anal. **3** (2013), 1460–1494.

[5] A. Lamacz, B. Schweizer, *A negative index meta-material for Maxwell's equations*, SIAM J. Math. Anal. **6** (2016), 4155–4174.

[6] J. Pendry, A. Holden, D. Robbins, W. Stewart *Magnetism from conductors and enhanced nonlinear phenomena*, IEEE Trans. Microwave Theory Tech. **47** (1999).

[7] V. Veselago *The electrodynamics of substances with simultaneously negative values of ε and μ*, Soviet Physics Uspekhi **10** (1968), 509–514.

On the curse of dimensionality for semilinear partial differential equations

Martin Hutzenthaler

(joint work with Weinan E, Thomas Kruse, Arnulf Jentzen, Tuan Ahn Nguyen, Philippe von Wurstemberger)

High-dimensional second-order partial differential equations (PDEs) are abundant in many important areas including financial engineering, economics, quantum mechanics, statistical physics, etc; see e.g. the surveys [7, 1]. Well-known examples are the nonlinear Black-Scholes equation in financial engineering for pricing financial

derivatives, the nonlinear Schrödinger equation in the many-body problem in quantum mechanics, the Hamilton-Jacobi-Bellman equation in stochastic control problems, and the dividend maximization problem in insurance mathematics. These PDEs are often nonlinear and high-dimensional. The challenge in the numerical approximation of solutions of high-dimensional nonlinear PDEs lies in the possible **curse of dimensionality** which means that the complexity of the problem goes up exponentially as a function of the dimension or of the inverse prescribed accuracy. Recently we discovered the full history recursive multilevel Picard method (MLP) in E et al. [6] and in Hutzenthaler et al. [11]. We extended and further studied this method analytically and numerically in [13, 12, 3, 8, 9, 2, 5, 10, 4]. Roughly speaking, MLP approximation methods are based on the idea, first, (I) to reformulate the PDE problem under consideration as a suitable stochastic fixed point equation, then, (II) to approximate the fixed point of the resulting stochastic fixed point equation through fixed point iterates, which in the context of temporal integral equations are referred to as Picard iterations, and, finally, (III) to approximate the expectations and the integrals appearing in the fixed point iterates through suitable multilevel Monte Carlo approximations.

References

[1] Bachmayr, M., Schneider, R., and Uschmajew, A. Tensor networks and hierarchical tensors for the solution of high-dimensional partial differential equations. *Foundations of Computational Mathematics 16*, 6 (2016), 1423–1472.

[2] Beck, C., Gonon, L., and Jentzen, A. Overcoming the curse of dimensionality in the numerical approximation of high-dimensional semilinear elliptic partial differential equations. *arXiv:2003.00596* (2020), 50 pages.

[3] Beck, C., Hornung, F., Hutzenthaler, M., Jentzen, A., and Kruse, T. Overcoming the curse of dimensionality in the numerical approximation of Allen-Cahn partial differential equations via truncated full-history recursive multilevel Picard approximations. *To appear in J. Numer. Math., arXiv:1907.06729* (2019), 31 pages.

[4] Beck, C., Jentzen, A., and Kruse, T. Nonlinear Monte Carlo methods with polynomial runtime for high-dimensional iterated nested expectations. *arXiv:2009.13989* (2020), 47 pages.

[5] Becker, S., Braunwarth, R., Hutzenthaler, M., Jentzen, A., and von Wurstemberger, P. Numerical simulations for full history recursive multilevel Picard approximations for systems of high-dimensional partial differential equations. *To appear in Commun. Comput. Phys., arXiv:2005.10206* (2020), 21 pages.

[6] E, W., Hutzenthaler, M., Jentzen, A., and Kruse, T. Multilevel Picard iterations for solving smooth semilinear parabolic heat equations. *arXiv:1607.03295v4* (2016).

[7] El Karoui, N., Peng, S., and Quenez, M. C. Backward stochastic differential equations in finance. *Mathematical finance 7*, 1 (1997), 1–71.

[8] Giles, M. B., Jentzen, A., and Welti, T. Generalised multilevel Picard approximations. *arXiv:1911.03188* (2019), 61 pages.

[9] Hutzenthaler, M., Jentzen, A., and Kruse, T. Overcoming the curse of dimensionality in the numerical approximation of parabolic partial differential equations with gradient-dependent nonlinearities. *arXiv:1912.02571* (2019), 33 pages.

[10] Hutzenthaler, M., Jentzen, A., Kruse, T., and Nguyen, T. A. Multilevel Picard approximations for high-dimensional semilinear second-order PDEs with Lipschitz nonlinearities. *arXiv:2009.02484* (2020), 37 pages.

[11] Hutzenthaler, M., Jentzen, A., Kruse, T., Nguyen, T. A., and von Wurstemberger, P. Overcoming the curse of dimensionality in the numerical approximation of semilinear parabolic partial differential equations. *arXiv preprint arXiv:1807.01212* (2018).
[12] Hutzenthaler, M., Jentzen, A., and von Wurstemberger, P. Overcoming the curse of dimensionality in the approximative pricing of financial derivatives with default risks. *Electron. J. Probab. 25* (2020), 73 pages.
[13] Hutzenthaler, M., and Kruse, T. Multilevel Picard approximations of high-dimensional semilinear parabolic differential equations with gradient-dependent nonlinearities. *SIAM J. Numer. Anal. 58*, 2 (2020), 929–961.

Error Analysis of a Mixed Discontinuous Galerkin Discretization for Maxwell Eigenvalue Problems in Periodic Media

Jacobus J.W. van der Vegt
(joint work with Zhongjie Lu, Yan Xu, Aycil Cesmelioglu, Kaifang Liu, M. Schlottbom, Devashish, Sjoerd Hack, Lars Corbijn van Willenswaard, Marek Kozon)

Numerical discretizations for the Maxwell equations need to address a number of important challenges: *i.*) the accurate computation of electromagnetic waves for long times and in large domains with minimal numerical dispersion and dissipation errors; *ii.*) the ability to deal with complex geometries, often containing small features (e.g. wires, thin layers, holes); *iii.*) the accurate computation of singularities at sharp corners, edges and material interfaces; *iv.*) the need for fast solvers, especially for the time-harmonic Maxwell equations (e.g. eigenvalue problems). During the last two decades Discontinuous Galerkin (DG) discretizations for the Maxwell equations have received significant interest since they present a novel way to address these challenges and provide an alternative to the frequently used finite difference time-domain, boundary integral and conforming finite element methods.

The use of basis functions in a DG methods that are discontinuous at element faces offers great flexibility in the development of *hp*-finite element discretizations that are well suited for mesh adaptation, e.g. to accurately compute singularities, and the approximation of complex geometries using general unstructured meshes. Also, parallel computing efficiency is greatly enhanced by the local element based structure of DG discretizations. DG methods have been demonstrated on large scale computations of electromagnetic waves, e.g. in [1, 4]. A detailed description of DG methods, including their theoretical analysis can be found in e.g. [3, 5]. A comprehensive analysis of various aspects of finite element methods for the Maxwell equations is presented in [8].

In this presentation we will focus on the error analysis of DG discretizations for the Maxwell eigenvalue problem in periodic media. Important examples of this class of problems are photonic crystals, which are lattice-like nanostructures with periodic electric permittivity [6]. For specific geometries, photonic crystals possess photonic band gaps in which the propagation of specific light frequencies through the crystal is prohibited. This can be used to control light propagation and emission, thus making photonic crystals very important for a wide range of photonic

applications [6]. However, designing and fabricating photonic crystals requires the knowledge of the frequencies at which light waves are completely reflected, propagated only in desired directions, or contained within a specified region, which asks for the solution of the Maxwell eigenvalue problem in periodic media. Solving the Maxwell eigenvalue problem poses, however, several challenges. In particular, one needs to ensure that the numerical discretization of the Maxwell eigenvalue problem converges to the exact eigenvalues and with the correct multiplicity, which questions are the main topic of this research.

In the computational modeling of photonic crystals we consider the following Maxwell eigenproblem:

$$\nabla \times (\epsilon^{-1} \nabla \times \mathbf{H}) = \omega^2 \mathbf{H} \qquad \text{in } \mathbb{R}^d, \tag{1a}$$

$$\nabla \cdot \mathbf{H} = 0 \qquad \text{in } \mathbb{R}^d, \tag{1b}$$

where the electric permittivity ϵ is periodic, and $\mathbf{H}$ is the magnetic field. This periodicity can be described mathematically by primitive lattice vectors $\{\mathbf{a}_i,\ i = 1, \cdots, d\}$, which form a maximal set of linearly independent vectors in $\mathbb{R}^d$ as follows:

$$\epsilon(\mathbf{x} + \mathbf{a}) = \epsilon(\mathbf{x}), \qquad \forall \mathbf{x} \in \mathbb{R}^d,$$

for any $\mathbf{a}$ that belongs to the Bravais lattice

$$A := \left\{ \sum_{i=1}^{d} k_i \mathbf{a}_i,\ k_i \in \mathbb{Z},\ i = 1, \cdots, d \right\}.$$

The periodic solution is now completely determined by its values on the primitive cell (fundamental domain), which is defined as

$$\Omega := \left\{ \mathbf{x} \in \mathbb{R}^d : \mathbf{x} = \sum_{i=1}^{d} x_i \mathbf{a}_i,\ x_i \in [0, 1],\ i = 1, \cdots, d \right\}.$$

Here we call $(\mathbf{H}, \omega^2)$ an eigenpair of problem (1). The Bloch waves are quasi-periodic functions satisfying

$$\mathbf{H}(\mathbf{x}) = e^{i\boldsymbol{\alpha}\cdot\mathbf{x}} \mathbf{u}(\mathbf{x}),$$

where $\mathbf{u}$ is periodic in $\mathbf{x}$, that is $\mathbf{u}(\mathbf{x} + \mathbf{a}) = \mathbf{u}(\mathbf{x})$, $\forall\ \mathbf{x} \in \mathbb{R}^d$, $\forall\ \mathbf{a} \in A$ and $\boldsymbol{\alpha}$ is in the associated first Brillouin zone K [6].

We assume that $\epsilon = \epsilon(\mathbf{x})$ is real and piecewise constant with respect to a partition of Ω, and there are real positive numbers $\epsilon_*, \epsilon^* > 0$ such that

$$0 < \epsilon_* \leq \epsilon(\mathbf{x}) \leq \epsilon^* < +\infty, \qquad \forall\ \mathbf{x} \in \overline{\Omega}.$$

By Bloch's theorem, we can transform the quasi-periodic problem (1) into a periodic problem. We introduce therefore the following shifted differential operators:

$$\nabla_{\boldsymbol{\alpha}} = \nabla + \boldsymbol{\alpha} i I,$$

where I is the identity operator and $i = \sqrt{-1}$. In order to explicitly enforce the constraint $\nabla_{\boldsymbol{\alpha}} \cdot \mathbf{u} = 0$ in the numerical discretization, we introduce a new variable

p as a Lagrange multiplier. The eigenvalue problem (1) then can be expressed as: for all $\boldsymbol{\alpha} \in K$, find $(\mathbf{u}, p, \omega^2)$, such that

$$\nabla_{\boldsymbol{\alpha}} \times (\epsilon^{-1} \nabla_{\boldsymbol{\alpha}} \times \mathbf{u}) - \nabla_{\boldsymbol{\alpha}} p = \omega^2 \mathbf{u} \qquad \text{in } \Omega, \tag{2a}$$

$$\nabla_{\boldsymbol{\alpha}} \cdot \mathbf{u} = 0 \qquad \text{in } \Omega, \tag{2b}$$

on the unit cell Ω with periodic boundary conditions $\mathbf{u}(\mathbf{x}+\mathbf{a}) = \mathbf{u}(\mathbf{x})$ and $p(\mathbf{x}+\mathbf{a}) = p(\mathbf{x})$ for all $\mathbf{x} \in \mathbb{R}^d$ and $\mathbf{a} \in A$.

The Maxwell eigenvalue problem (2) in a unit cell Ω is solved using a mixed discontinuous Galerkin discretization. Given a finite element tessellation $\mathcal{T}_h$, we introduce the following finite element spaces:

$$Q_h^{\boldsymbol{\alpha}} = \{\phi \in L^2(\Omega) \ : \ \phi_K = e^{-i\boldsymbol{\alpha}\cdot\mathbf{x}} \tilde{\phi} \text{ for some } \tilde{\phi} \in \mathcal{P}_{k+1}(K) \ \forall K \in \mathcal{T}_h\},$$
$$\mathbf{V}_h^{\boldsymbol{\alpha}} = \{\mathbf{v} \in \mathbf{L}^2(\Omega) \ : \ \mathbf{v}_K = e^{-i\boldsymbol{\alpha}\cdot\mathbf{x}} \tilde{\mathbf{v}} \text{ for some } \tilde{\mathbf{v}} \in \mathcal{S}_k(K) \ \forall K \in \mathcal{T}_h\},$$

where $L^2(\Omega)$ is the space of square integral functions on Ω, $\mathcal{P}_k(K)$ is the set local polynomials of degree less than or equal to k on K; the elements in $\mathcal{S}_k(K)$ have the form $\mathbf{a}(\mathbf{x}) + \mathbf{b}(\mathbf{x}) \times \mathbf{x}$, with $\mathbf{a}, \mathbf{b} \in \mathcal{P}_k(K)^3$.

Let $\mathcal{T}_h$ be a periodic, shape-regular, conformal mesh on Ω aligned with the possible discontinuities of ϵ. We denote the set of all faces of $\mathcal{T}_h$ by $\mathcal{F}_h$, the set of boundary faces $\mathcal{F}_h^b = \mathcal{F}_h \cap \partial\Omega$ and the set of interior faces $\mathcal{F}_h^i = \mathcal{F}_h \backslash \mathcal{F}_h^b$.

For functions that are discontinuous on element faces, we define jumps and averages across a face $f \in \mathcal{F}_h$ as follows: If $f \in \mathcal{F}_h$ is shared by tetrahedra $K_\pm \in \mathcal{T}_h$ with unit outward normal vectors $\mathbf{n}_\pm$, we define, respectively, the tangential and normal jumps and the average of $\mathbf{v}$ across the interior face $f \in \mathcal{F}_h^i$ as:

$$[[\mathbf{v}]]_T := \mathbf{n}_+ \times \mathbf{v}_+ + \mathbf{n}_- \times \mathbf{v}_-, \ [[\mathbf{v}]]_N := \mathbf{n}_+ := \mathbf{v}_+ + \mathbf{n}_- := \mathbf{v}_-, \ \{\{\mathbf{v}\}\} := \frac{\mathbf{1}}{\mathbf{2}}(\mathbf{v}_+ + \mathbf{v}_-),$$

and we define the normal jump and average of q as:

$$[[q]]_N = \mathbf{n}_+ q_+ + \mathbf{n}_- q_-, \qquad \{\{q\}\} = \frac{1}{2}(q_+ + q_-),$$

where $\mathbf{v}_\pm$ denote the traces of $\mathbf{v}$ taken from within $K_\pm$. At the boundary, we define the jumps and means in a periodic way.

For $\boldsymbol{\alpha} \in K$, with $\boldsymbol{\alpha} \neq \mathbf{0}$, we introduce the following mixed DG method: find $(\mathbf{u}_h, p_h, \omega_h^2) \in \mathbf{V}_h^{\boldsymbol{\alpha}} \times Q_h^{\boldsymbol{\alpha}} \times \mathbb{C}$ with $(\mathbf{u}_h, p_h) \neq (\mathbf{0}, 0)$, such that

$$\begin{aligned} a_h(\mathbf{u}_h, \mathbf{v}) + b_h(\mathbf{v}, p_h) &= \omega_h^2 (\mathbf{u}_h, \mathbf{v}), \\ \overline{b_h(\mathbf{u}_h, q)} - c_h(p_h, q) &= 0, \end{aligned} \tag{3}$$

for all $(\mathbf{v}, q) \in \mathbf{V}_h^{\boldsymbol{\alpha}} \times Q_h^{\boldsymbol{\alpha}}$, where the discrete forms a_h, b_h and c_h are defined as follows:

$$\begin{aligned} a_h(\mathbf{u}, \mathbf{v}) := & \int_\Omega \epsilon^{-1} \nabla_{\boldsymbol{\alpha},h} \times \mathbf{u} \cdot \overline{\nabla_{\boldsymbol{\alpha},h} \times \mathbf{v}} d\mathbf{x} - \int_{\mathcal{F}_h} [[\mathbf{u}]]_T \cdot \overline{\{\{\epsilon^{-1} \nabla_{\boldsymbol{\alpha},h} \mathbf{v}\}\}} ds \\ & - \int_{\mathcal{F}_h} \overline{[[\mathbf{v}]]}_T \cdot \{\{\epsilon^{-1} \nabla_{\boldsymbol{\alpha},h} \times \mathbf{u}\}\} ds + \int_{\mathcal{F}_h} a_F [[\mathbf{u}]]_T \cdot \overline{[[\mathbf{v}]]}_T ds \\ & + \int_{\mathcal{F}_h} b_F [[\mathbf{u}]]_N \overline{[[\mathbf{v}]]}_N ds, \\ b_h(\mathbf{v}, p) := & - \int_\Omega \overline{\mathbf{v}} \cdot \nabla_{\boldsymbol{\alpha},h} p d\mathbf{x} + \int_{\mathcal{F}_h} \overline{\{\{\mathbf{v}\}\}} \cdot [[p]]_N ds, \\ c_h(p, q) := & \int_{\mathcal{F}_h} c_F [[p]]_N \cdot \overline{[[q]]}_N ds. \end{aligned}$$

The main steps in the error analysis can now be summarised as:

(1) Proof continuity and semi-ellipticity of $a_h(\cdot, \cdot)$.
(2) Rewrite the eigenvalue problem in the standard form for mixed methods and proof an inf-sup condition for the mixed formulation.
(3) Derive an a priori error bound and proof uniform convergence of the numerical solution operator.
(4) Use the spectral approximation theory in [2] and the results from step (3) to obtain bounds on the error in the eigenvalues and eigenfunctions.

The result of this analysis is that

$$|\omega^2 - \omega_h^2| \leq C h^{2 \min\{s, k+1\}},$$

with k the polynomial order of the basis functions and s the regularity of the solution. The error in the eigenfunctions is proportional to $h^{\min\{s,k+1\}}$. For the full details of the analysis we refer to [7].

References

[1] E. Agullo, L. Giraud, A. Gobé, M. Kuhn, S. Lanteri, *High order HDG method and domain decomposition solvers for frequency-domain electromagnetics.* Int. J. Numer. Model. 33:e2678 (2020).

[2] J. Descloux, N. Nassif, J. Rappaz *On spectral approximation. Part1. The problem of convergence.* RAIRO-Anal. Num. 12(2):97-112 (1978).

[3] D.A. DiPietro, A. Ern, Mathematical aspects of discontinuous Galerkin methods, Springer 2012.

[4] J.S. Hesthaven, T. Warburton, *High-order accurate methods for time-domain electromagnetics.* Comput. Model. Engr. Sci. 5 (5), 395-408 (2004).

[5] J.S. Hesthaven, T. Warbuton, Nodal discontinuous Galerkin methods. Algorithms, Analysis, and Applications, Springer, 2008.

[6] J.D. Joannopoulos, S.G. Johnson, J.N. Winn, R.D. Meade, Photonic Crystals. Molding the flow of light, 2nd ed. Princeton University Press, 2008.

[7] Z. Lu, A. Cesmelioglu, J.J.W. van der Vegt, Yan Xu, *Discontinuous Galerkin approximations for computing electromagnetic Bloch modes in photonics crystals.* J. Sci. Comput., 70:922-964 (2017).
[8] P. Monk, Finite element methods for Maxwell's equations, Oxford Science Publications, 2003.

Mixed discontinuous Galerkin discretization of the time-harmonic Maxwell equations with minimal smoothness requirements

Kaifang Liu

(joint work with D. Gallistl, M. Schlottbom and J.J.W. van der Vegt)

Problems. We consider the analysis of mixed discontinuous Galerkin approximations for the time-harmonic Maxwell equations with low regularity solutions: find $\mathbf{u}, p$ such that

$$\nabla \times (\mu^{-1}\nabla \times \mathbf{u}) - k^2\varepsilon\mathbf{u} - \varepsilon\nabla p = \mathbf{j} \quad \text{in } \Omega, \tag{1a}$$

$$\nabla \cdot (\varepsilon\mathbf{u}) = 0 \quad \text{in } \Omega, \tag{1b}$$

$$\mathbf{n} \times \mathbf{u} = \mathbf{0} \quad \text{on } \Gamma, \tag{1c}$$

$$p = 0 \quad \text{on } \Gamma. \tag{1d}$$

Here, $\mathbf{u}$ represents the electrical field, p the Lagrange multiplier used to enforce the divergence constraint (1b), k is the wave number and $\mathbf{j} \in L^2(\Omega)^3$ is the source term. The piecewise constant coefficients μ and ε are the magnetic permeability and electrical permittivity of the media, respectively. We assume that $\Omega \subset \mathbb{R}^d$, $d = 2, 3$ is a simply connected Lipschitz domain with connected boundary Γ and $\mathbf{n}$ is the external unit normal vector. In general, problem (1) admits solutions with $\mathbf{u}$ s.t. $\mathbf{u}, \nabla \times \mathbf{u} \in H^s(\Omega)$, where $s > 0$ could be arbitrarily close to zero, which causes difficulties for nonconforming discretizations and error analysis.

Backgrounds and difficulties. The key difficulty in the error analysis of nonconforming FEMs for non-smooth problems is that the classical trace theorems are not applicable, i.e., the exact solution does not have a sufficiently regular trace on mesh faces. Until now, only a few techniques have been developed to overcome this difficulty. One technique for the Maxwell equations relies on the definition of generalized traces [3, Proposition 7.3 and Assumption 4]. In the spirit of [3], [4] proposed an interior-penalty method with C^0 finite elements for the Maxwell equations with minimal smoothness requirements. Recently, [6] analyzed a nonconforming approximation of elliptic PDEs with minimal regularity by introducing a generalized normal derivative of the exact solution at the mesh faces. They also showed that this idea can be extended to solve the time-harmonic Maxwell equations with low regularity solutions by introducing a more general concept for the tangential trace. Another technique that avoids the definition of generalized traces, which has been proposed by [7] in the context of elliptic PDEs, is to use an enriching map to transform a non-conforming function into a conforming one. It is well-known that stabilization of interior-penalty discontinuous Galerkin methods, in general, requires a sufficiently large penalty parameter, while there is no

explicit formula for computing the parameter and this causes some trouble in applications. A remedy follows from the idea of DG for turbomachinery flows and elliptic problems, see, e.g. [1, 2], where the lifting operator is used to replace the integral on faces by an integral on volumes and get the stabilization of DG for an explicit and computable parameter.

Aims and techniques. In this work, we analyse a mixed DG formulation for the Maxwell equations with low regularity solutions, which modifies the method of [8] by using lifting operator [2] and we aim to obtain

- an explicit expression for stabilization parameters;
- A priori error estimates of mixed DG method under low regularity:

$$\varepsilon\mathbf{u} \in H^r(\mathcal{T}_h)^3,\ \mu^{-1}\nabla\times\mathbf{u} \in H^r(\mathcal{T}_h)^3$$

  with exponent $r > 0$, which could be arbitrarily close to zero;
- A quantitative convergence statement of the mixed DG approximation for low regularity solutions.

The main objective is to generalize the error analysis of [8] to the non-smooth case and to present optimal a priori error estimates for the low regularity solution in the broken Sobolev space $H^s(\mathcal{T}_h), s \geq 0$ with $\mathcal{T}_h$ the finite element partition. The proof of our a priori error analysis is different from [3, 6] in that, first, it employs a lifting operator that allows us to replace integrals over faces by integrals over volumes and, thus, avoids the definition of a generalized tangential trace on mesh faces. A further major benefit of using the lifting operator is that we obtain an explicit expression for stabilization parameters, which, compared to [8], facilitates the implementation considerably. Secondly, we use smoothed interpolations [5], which map low regularity solutions to corresponding conforming finite element spaces, and generalize the residual equations for low regularity solutions, and finally, combined with the best approximation obtained by a newly defined quasi-interpolation, to prove optimal convergence rates.

References

[1] Bassi, F., Rebay, S., Mariotti, G., Pedinotti, S., and Savini, M. *A high order accurate discontinuous finite element method for inviscid and viscous turbomachinery flows.* Proceedings of the 1997 2nd European Conference on Turbomachinery - Fluid Dynamics and Thermodynamics, Antwerpen, Belgium, (1997), 99–108.

[2] Brezzi, F., Manzini, G., Marini, D., Pietra, P., and Russo, A. *Discontinuous Galerkin approximations for elliptic problems.* Numerical Methods for Partial Differential Equations: An International Journal, (2000), 16(4), 365–378.

[3] Buffa, A., and Perugia, I. *Discontinuous Galerkin approximation of the Maxwell eigenproblem.* SIAM J. Numer. Anal., (2006), 44(5), 2198–2226.

[4] Bonito, A., Guermond, J.-L., and Luddens, F. *An interior penalty method with C^0 finite elements for the approximation of the Maxwell equations in heterogeneous media: convergence analysis with minimal regularity.* ESAIM: M2NA, (2016), 50(5), 1457–1489.

[5] Ern, A., and Guermond, J.-L. Mollification in Strongly Lipschitz Domains with Application to Continuous and Discrete De Rham Complexes. Comput. Methods in Appl. Math., (2016), 16(1), 51–75.

[6] Ern, A., and Guermond, J.-L. (2019). Quasi-optimal nonconforming approximation of elliptic PDEs with contrasted coefficients and minimal regularity. ArXiv.org.

[7] Gudi, T. *A new error analysis for discontinuous finite element methods for linear elliptic problems*. Math. Comput., (2010), 79(272), 2169–2169.
[8] Houston, P., Perugia, I., and Schötzau, D. *Mixed discontinuous Galerkin approximation of the Maxwell operator*. SIAM J. Numer. Anal., (2004), 42(1), 434–459.

Toward accurate and efficient boundary integral equation methods for metasurface design

Carlos Pérez-Arancibia
(joint work with Raphaël Pestourie, Rodrigo Arrieta, and Steven G. Johnson)

We consider a class of electromagnetic scattering problems arising in the design of optical metasurfaces. Metasurfaces are planar metamaterial slabs of subwavelength thickness consisting of a pattern made up of a large number of subwavelength optical elements (typically, nanorods or nanopillars), that are engineered to manipulate the direction, amplitude, phase, and polarization of light [1]. The massive size and multiple-scale complexity of the computational domains involved in these problems pose major challenges to general-purpose PDE solvers, hence opening up exciting research opportunities for the development of efficient physics-informed numerical approximations and/or for the improvement of specialized Maxwell/Helmholtz solvers.

In the first part of our talk, we present a PDE-constrained adjoint-based optimization framework for metasurface inverse design [2] that relies on a fast but low-order scattering approximation—known as the *locally-periodic approximation* (LPA)—which is used to avoid fully solving the governing Maxwell equations at each step of the iterative optimization solver. The LPA, which can be cast as an embarrassingly parallel domain decomposition method, leverages the often slow variation of the design parameters (e.g., cross-section radius, semi-axis length) that define the shape of the optical elements, to reduce the full solution to a small number of independent unit-cell periodic problems. The scattered field LPA is then constructed via a Chebyshev surrogate model and a suitable Green's integral representation formula that suitably combines the local near fields to produce the far-field at the desired locations. We present a variety of examples that demonstrate both the capabilities and the limitations of the LPA. Indeed, examples of metasurfaces are shown in which the LPA fails to provide accurate enough solutions and where difficult-to-compute higher-order corrections are needed to properly account for the relevant physics [3]. These examples reveal, in part, that despite the success of the LPA in some settings, provably accurate full-wave solutions are still very valuable either for validation of optimized designs, for the training of surrogate models, or for optimization (provided an appropriate balance between accuracy and speed is considered).

In the second part of our talk, we present an efficient high-order boundary integral equation (BIE) method for the full-wave numerical solution of metasurface scattering problems. We first frame them as classical locally perturbed two-layer media scattering problems for which well-posedness has been established in [4], and

we justify the use of BIE methods for their solution over finite difference and finite element methods. Emphasis is given on the salient limitations of standard layered media BIE methods based on Sommerfeld integrals (see, e.g., [5]) that (arguably) render metasurface scattering problems intractable by them. We then introduce a fast, flexible, and easy-to-implement BIE method based on the windowed Green function (WGF) method [6, 7, 8, 9]. Unlike standard approaches, the proposed methodology does not involve the evaluation of computationally expensive Sommerfeld integrals as it leverages a BIE formulation given in terms of free-space Green functions that involves integration over the entire unbounded penetrable boundary. The unbounded BIE domain is effectively reduced to a small-area surface using the WGF method, which exhibits high-order (super-algebraic) convergence as the size of the truncated surface increases. The resulting (second-kind) windowed integral equation can be numerically solved by means of off-the-shelf BIE methods. A variety of examples demonstrate the applicability, accuracy, and efficiency (as compared to the Sommerfeld-integral approach) of the proposed methodology based on both spectrally-accurate Nyström and boundary element methods. Promising results are shown, where, to the best of the author's knowledge, a full-wave 3D BIE solver has for the first time been used to compute the electromagnetic scattering off of a small-size light-focusing all-dielectric metasurface [10].

References

[1] N. Yu and F. Capasso, *Flat optics with designer metasurfaces*, Nature Materials **13(2)** (2014), 139–150.

[2] R. Pestourie, C. Pérez-Arancibia, Z. Lin, W. Shin, F. Capasso, and S. G. Johnson, *Inverse design of large-area metasurfaces*, Optics Express **26:26** (2018), 33732–33747.

[3] C. Pérez-Arancibia, R. Pestourie, and S. G. Johnson, *Sideways adiabaticity: Beyond ray optics for slowly varying metasurfaces*, Optics Express **26(23)** (2018), 30202–30230.

[4] P. M. Cutzach and C. Hazard, *Existence, uniqueness and analyticity properties for electromagnetic scattering in a two-layered medium*, Mathematical Methods in the Applied Sciences **21(5)** (1998), 433–461.

[5] W. Cai, *Algorithmic issues for electromagnetic scattering in layered media: Green's functions, current basis, and fast solver*, Advances in Computational Mathematics **16(2)** (2002), 157–174.

[6] C. Pérez-Arancibia, Windowed integral equation methods for problems of scattering by defects and obstacles in layered media, Ph.D. thesis, California Institute of Technology (2016).

[7] O. P. Bruno, M. Lyon, C. Pérez-Arancibia, and C. Turc, *Windowed Green function method for layered-media scattering*, SIAM Journal on Applied Mathematics **76(5)** (2016), 1871–1898.

[8] O. P. Bruno and C. Pérez-Arancibia, *Windowed Green function method for the Helmholtz equation in the presence of multiply layered media*, Proceedings of the Royal Society A: Mathematical, Physical and Engineering Sciences **473(2202)** (2017), 20170161.

[9] O. P. Bruno, E. Garza, and C. Pérez-Arancibia, *Windowed Green function method for nonuniform open-waveguide problems*, IEEE Transactions on Antennas and Propagation **65(9)** (2017), 4684–4692.

[10] R. Arrieta and C. Pérez-Arancibia, *Windowed Green function method of moments for electromagnetic scattering by layered media*. Submitted (available on ResearchGate) (2021).

Least-Squares and dPG methods with edge finite elements for the approximation of eigenvalues

Henrik Schneider
(joint work with Fleurianne Bertrand)

Edge finite elements are the natural choice for the approximation of the Maxwell eigenvalues. In the framework of mixed methods, they allow for rotation-based variational formulations involving the rotation as an independent variable approximated in a suitable $H(\mathrm{curl})$-conforming finite element spaces. Such approaches may either lead to a saddle-point problem or to a symmetric positive definite system. The approximation of eigenvalue with saddle-point problems have been intensively studied and we refer to [2] for an overview. This talk, therefore, focuses on methods leading to symmetric positive definite systems. This includes the Least-Squares method (see [3] for a comprehensive overview) and the discontinuous Petrov-Galerkin method, introduced in a series of papers [4, 5, 6].

1. Computation of the eigenvalues with the Least-Squares method

The recently published articles [1, 7, 8] investigate the Least-Squares finite element approximation of the eigensolutions of operators associated with second-order elliptic equations. Given $f \in L^2(\Omega)$, the simplest Least-Squares formulation for the source problem $-\mathrm{curl}\ \mathbf{curl}\ u = f$ with boundary conditions $\mathbf{curl}\ u \times \mathbf{n} = 0$, is given by the minimization of the functional

$$\mathcal{F}(\boldsymbol{\tau}, v) = \|\boldsymbol{\tau} - \mathbf{curl}\ v\|^2 + \|\mathrm{curl}\ \boldsymbol{\tau} + f\|^2.$$

The rotation $\boldsymbol{\sigma} = \mathbf{curl}\ u$ belongs to the space $\mathbf{H}_0(\mathrm{curl};\Omega)$ consisting of the functions $\boldsymbol{\tau}$ in $L^2(\Omega)^2$ with $\mathrm{curl}\ \boldsymbol{\tau} \in L^2(\Omega)$ and $\boldsymbol{\tau} \times \mathbf{n} = 0$ on $\partial\Omega$. The corresponding variational formulation can be used in a natural way to consider the following eigenvalue problem: find $\lambda \in \mathbb{C}$ and $u \in H^1(\Omega)$ with $u \neq 0$ and $(u, 1) = 0$ such that for some $\boldsymbol{\sigma} \in \mathbf{H}_0(\mathrm{curl};\Omega)$ it holds

$$\begin{cases} (\boldsymbol{\sigma}, \boldsymbol{\tau}) + (\mathrm{curl}\,\boldsymbol{\sigma}, \mathrm{curl}\,\boldsymbol{\tau}) - (\mathbf{curl}\ u, \boldsymbol{\tau}) = -\lambda(u, \mathrm{curl}\,\boldsymbol{\tau}) & \forall \boldsymbol{\tau} \in \mathbf{H}_0(\mathrm{curl};\Omega) \\ -(\boldsymbol{\sigma}, \mathbf{curl}\ v) + (\mathbf{curl}\ u, \mathbf{curl}\ v) = 0 & \forall v \in H^1(\Omega),\ (v,1) = 0 \end{cases}$$

Let $\Sigma_h \subset \mathbf{H}_0(\mathrm{curl};\Omega)$ and $U_h \subset H^1(\Omega)$ be conforming finite element spaces. The discretization of (1) reads: find $\lambda_h \in \mathbb{R}$ and $u_h \in U_h$ with $u_h \neq 0$ and $(u_h, 1) = 0$ such that for some $\boldsymbol{\sigma}_h \in \Sigma_h$ it holds

$$\begin{cases} (\boldsymbol{\sigma}_h, \boldsymbol{\tau}) + (\mathrm{curl}\,\boldsymbol{\sigma}_h, \mathrm{curl}\,\boldsymbol{\tau}) - (\mathbf{curl}\ u_h, \boldsymbol{\tau}) = -\lambda_h(u_h, \mathrm{curl}\,\boldsymbol{\tau}) & \forall \boldsymbol{\tau} \in \Sigma_h \\ -(\boldsymbol{\sigma}_h, \mathbf{curl}\ v) + (\mathbf{curl}\ u_h, \mathbf{curl}\ v) = 0 & \forall v \in U_h, (v_h, 1) = 0 \end{cases}$$

Regarding the source problem, the choice of finite element spaces for the approximation of the different variables is not restricted by compatibility conditions. However, for the eigenvalue problem, our framework is restricted to finite element

spaces Σ_h and U_h satisfying the following approximation properties

$$\inf_{\boldsymbol{\tau}\in\Sigma_h} \|\boldsymbol{\chi}-\boldsymbol{\tau}\|_{\mathbf{H}_0(\mathrm{curl};\Omega)} \leq Ch^s \left(\|\boldsymbol{\chi}\|_{\mathbf{H}^s(\Omega)} + \|\operatorname{div}\boldsymbol{\chi}\|_{H^{1+s}(\Omega)}\right)$$
$$\inf_{v\in U_h} \|p-v\|_{H^1(\Omega)} \leq Ch^s \|p\|_{H^{1+s}(\Omega)}$$

Using duality arguments, we are then able to derive refined L^2-estimates that directly imply the uniform convergence of the discrete solution operator to the continuous one and thus, the convergence of the eigenvalues.

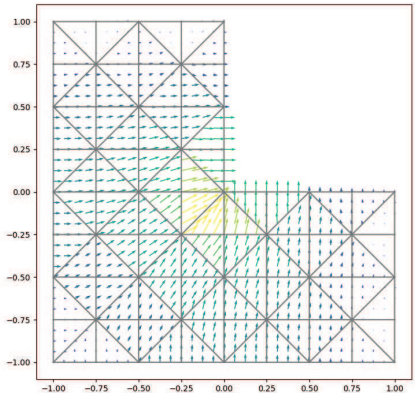

FIGURE 1. Approximation of the first eigenfunction on the L-shape with edge finite elements

2. Computation of the eigenvalues with the discontinuous Petrov-Galerkin method

The discontinuous Petrov-Galerkin method was originally constructed to find optimal discrete test functions to get optimal stability constants. The method can be charaterised as a mixed and Least-Squares method. Since it is not pratical to compute the optimal test functions for every class of problems the practical dPG formulation [9] was introduced, with easily computable test-spaces which are arbitrary close to the optimal ones. The mixed formulation of the dPG method comes also with a residual error estimator, that can be used for an hp adaptive scheme. Normally, the trial space U can be split into two parts, where the first one U_0 represents the volumetric part and the second U_1 the remaining components. Usually, U_1 contains functions that are defined on the hole domain Ω, as well as those which are only defined on the skeleton of the triangulation $\mathcal{T}$. So the continuous eigenvalue problem reads: find eigenvalues $\lambda \in \mathbb{C}$ and eigenfunctions $u = (u_0, u_1) \in U = U_0 \times U_1$ with $u_0 \neq 0$ such that

$$b(u,v) = \lambda m(u_0, v) \quad \forall v \in V.$$

In general the two space U and V are not the same. Since the mixed formulation is suitable for computation, we use this form to present the discrete problem. Let

$U_h \subset U$ and $V \subset V_h$, then the problem reads: find $\lambda_h \in \mathbb{C}$ such that for some $u_h = (u_{0,h}, u_{1,h}) \in U_h = U_{0,h} \times U_{1,h}$ with $u_{0,h} \neq 0$ and some $\varepsilon_h \in V_h$ it holds

$$\begin{cases} (\varepsilon_h, v_h)_V + b(u_h, v_h) = \lambda_h m(u_{0,h}, v_h) & \forall v_h \in V_h \\ \overline{b(z_h, \varepsilon_h)} = 0 & \forall z_h \in U_h. \end{cases}$$

By using the Babŭska–Osborn theory [10] and the known convergence results for the source problem we can prove the uniform convergence of the eigenvalues for a primal and ultra-weak formulation. The included error estimator is connected with the energy residual $\|\varepsilon_h\|$. For this estimator, we can prove global efficiency and reliability, where these estimates are dependent on the usually higher-order term $\lambda u_0 - \lambda_h u_{0,h}$. In Figure 2 the results of the computation of the first ten eigenvalues are presented. The computation of the eigenvalues was performed by an iterative solver and so all eigenvalues have and complex part in the range of the machine epsilon. The chosen mesh a criss-cross triangulation of the square, at which for some methods so-called spurious eigenfunction occurs which is not the case here.

Exact	Computed			
1	1.31601	1.08121	1.02034	1.00509
1	1.31601	1.08121	1.02034	1.00509
2	2.69169	2.18003	2.04501	2.01125
4	5.1988	4.74426	4.18535	4.04613
4	5.1988	4.74426	4.18535	4.04613
5	6.87823	5.90737	5.22378	5.05556
5	6.87823	5.90737	5.22378	5.05556
8	-	9.84221	8.44574	8.10981
9	-	12.0643	9.8114	9.2009
9	-	12.0643	9.81144	9.20122
DoF	147	567	2223	8799

FIGURE 2. Real part of the computed eigenvalues with the primal formulation

REFERENCES

[1] Alzaben, L. and Bertrand, F. and Boffi, D., *Computation of Eigenvalues in Linear Elasticity with Least-Squares Finite Elements: Dealing with the Mixed System*, 01/2021, 10.23967/wccm-eccomas.2020.095.

[2] Boffi, D. *Finite element approximation of eigenvalue problems*, Acta Numer. **19** (2010), 1–120.

[3] Bochev, P. and Gunzburger, M. *A Locally Conservative Least-Squares Method for Darcy Flows*, Commun. Numer. Meth. Engrg **24** (2008), 97–110.

[4] Demkowicz, L. and Gopalakrishnan, J. *A class of discontinuous Petrov-Galerkin methods. Part I: the transport equation*, Comput. Methods Appl. Mech. Engrg. **199** (2010), 1558–1572.

[5] Demkowicz, L. and Gopalakrishnan, J., *A class of discontinuous Petrov-Galerkin methods. II. Optimal test functions*, Numer. Methods Partial Differential Equations **27** (2011), 70–105.
[6] Demkowicz, L. and Gopalakrishnan, J. and Niemi, A. H. *A class of discontinuous Petrov-Galerkin methods. Part III: Adaptivity* Appl. Numer. Math. **62** (2012), 496–427.
[7] Bertrand, F. and Boffi, D. *First order Least-Squares formulations for eigenvalue problems* accepted for publication in IMA.
[8] Bertrand, F. and Boffi, D. *Least-Squares for linear elasticity eigenvalue problem* accepted for publication in CAMWA.
[9] Gopalakrishnan, J. and Qiu, W., *An analysis of the practical DPG method*, Math. Comp. **83** (2014), 537—552.
[10] Babuška, I. and Osborn, J., *Eigenvalue problems*, Handbook of numerical analysis, Vol. **II** (1991), 641–787.
[11] Carstensen, C. and Demkowicz, L. and Gopalakrishnan,J., *A posteriori error control for DPG methods*, SIAM J. Numer. Anal. **52** (2014), 1335–1353.

Towards a metriplectic structure for radiative transfer equations

Matthias Schlottbom
(joint work with Michael Kraus)

Transport of electromagnetic radiation has many important applications, such as medical imaging [1], climate sciences [2] and in geosciences [10]. In these applications, the high complexity of the scattering media in terms of number and geometry of scatterers does not allow to directly simulate Maxwell's equations [7],

$$\frac{\partial \mathbf{E}}{\partial t} = \frac{1}{\varepsilon}\nabla \times \mathbf{H}, \qquad \frac{\partial \mathbf{H}}{\partial t} = -\frac{1}{\mu}\nabla \times \mathbf{E}.$$

Here, $\varepsilon(\mathbf{x})$ denotes the spatially varying dielectric permittivity, $\mu(\mathbf{x})$ the relative magnetic permeability, and $\mathbf{E}$ and $\mathbf{H}$ are the electric and magnetic field, respectively. Instead, the radiative transfer equation (RTE) has been established as a sound physical model by a rigorous derivation from Maxwell's equations [3, 9].

In the following, we discuss the case without polarization, which leaves us with the following radiative transfer equation for the specific intensity $\rho(\mathbf{x}, \mathbf{k}, t)$,

$$\frac{\partial \rho}{\partial t} = \nabla_{\mathbf{x}}\omega \cdot \nabla_{\mathbf{k}}\rho - \nabla_{\mathbf{k}}\omega \cdot \nabla_{\mathbf{x}}\rho + \int_{|\mathbf{k}'|=|\mathbf{k}|} \sigma(.,\mathbf{k}'\cdot\mathbf{k})\rho(.,\mathbf{k}',.)\mathrm{d}S(\mathbf{k}') - \Sigma\rho \tag{1}$$

for the phase space variables $(\mathbf{x}, \mathbf{k}) \in \mathbb{R}^3 \times \mathbb{R}^3$ and $\mathrm{d}S$ denoting surface integration. The dispersion relation is $\omega(\mathbf{x}, \mathbf{k}) = v(\mathbf{x})|\mathbf{k}|$, with $v(\mathbf{x}) = 1/\sqrt{\varepsilon(\mathbf{x})\mu(\mathbf{x})}$ denoting the speed of light. The differential scattering cross section $\sigma(\mathbf{x}, \mathbf{k}'\cdot\mathbf{k}) > 0$, which describes the probability of post-collisional direction $\mathbf{k}$ given pre-collisional direction $\mathbf{k}'$, satisfies the normalization condition

$$\int_{|\mathbf{k}'|=|\mathbf{k}|} \sigma(\mathbf{x}, \mathbf{k}'\cdot\mathbf{k})\mathrm{d}S(\mathbf{k}') = \Sigma(\mathbf{x}, |\mathbf{k}|). \tag{2}$$

Scattering is introduced by random fluctuations of the medium. Without these fluctuations, $\sigma = 0$ and (1) is the Liouville equation of geometric optics.

Abstract metriplectic dynamics. Metriplectic dynamics are a formalism to describe dynamical systems that contain Hamiltonian and dissipative dynamics [4, 5, 8]. The evolution of a functional $\mathcal{F}$ of the dynamical variables is given by

$$\frac{\mathrm{d}\mathcal{F}}{\mathrm{d}t} = \{\mathcal{F}, \mathcal{G}\} + (\mathcal{F}, \mathcal{G})\,, \tag{3}$$

where $\mathcal{G} = \mathcal{H} + \mathcal{S}$ is a free energy functional with total energy $\mathcal{H}$ and entropy $\mathcal{S}$. The most important properties for our discussion are that the Poisson bracket $\{\cdot,\cdot\}$ is bilinear and anti-symmetric, while the metric bracket $(\cdot,\cdot)$ is bilinear, symmetric negative semi-definite. Employing the basic assumptions that $\{\mathcal{A}, \mathcal{S}\} = 0$ and $(\mathcal{A}, \mathcal{H}) = 0$ for all functionals $\mathcal{A}$, that is $\mathcal{S}$ and $\mathcal{H}$ are Casimirs of the respective brackets, the first and second law of thermodynamics are guaranteed, i.e., conservation of energy and dissipation of entropy

$$\frac{\mathrm{d}\mathcal{H}}{\mathrm{d}t} = \{\mathcal{H}, \mathcal{G}\} + (\mathcal{H}, \mathcal{G}) = 0, \qquad \frac{\mathrm{d}\mathcal{S}}{\mathrm{d}t} = \{\mathcal{S}, \mathcal{G}\} + (\mathcal{S}, \mathcal{G}) \leq 0.$$

The RTE as a metriplectic system. Denoting the canonical Poisson bracket by $[f, g] = \nabla_{\mathbf{x}} f \cdot \nabla_{\mathbf{k}} g - \nabla_{\mathbf{k}} f \cdot \nabla_{\mathbf{x}} g$ and the L^2-gradient of a functional $\mathcal{A}$ by $\frac{\delta \mathcal{A}}{\delta \rho}$, we define a Poisson and a metric bracket for functionals as follows

$$\{\mathcal{A}, \mathcal{B}\} = \int_{\mathbb{R}^3}\int_{\mathbb{R}^3} \rho \left[\frac{\delta \mathcal{A}}{\delta \rho}, \frac{\delta \mathcal{B}}{\delta \rho}\right] \mathrm{d}\mathbf{k}\,\mathrm{d}\mathbf{x},$$

$$(\mathcal{A}, \mathcal{B}) = \int_{\mathbb{R}^3}\int_{\mathbb{R}^3}\int_{|\mathbf{k}'|=|\mathbf{k}|} \sigma(\mathbf{x}, \mathbf{k}'\cdot\mathbf{k}) \frac{\delta \mathcal{A}}{\delta \rho'}\Big(\frac{\delta \mathcal{B}}{\delta \rho} - \frac{\delta \mathcal{B}}{\delta \rho'}\Big) \mathrm{d}S(\mathbf{k}')\,\mathrm{d}\mathbf{k}\,\mathrm{d}\mathbf{x}.$$

Here, $\frac{\delta \mathcal{A}}{\delta \rho'}$ means that $\frac{\delta \mathcal{A}}{\delta \rho}$ is evaluated at $\mathbf{k}'$. Clearly, the Poisson bracket is bilinear and antisymmetric. Moreover, the particular form of $\sigma(\mathbf{x}, \mathbf{k}'\cdot\mathbf{k})$ implies that the metric bracket is symmetric. Using (2) and the Cauchy-Schwarz inequality, one can show that the metric bracket is negative semi-definite. Therefore, these two brackets fit the metriplectic framework outlined above.

The total energy is described by the Hamiltonian functional

$$\mathcal{H}[\rho](t) = \int_{\mathbb{R}^3}\int_{\mathbb{R}^3} \rho(\mathbf{x}, \mathbf{k}, t) v(\mathbf{x}) |\mathbf{k}|\,\mathrm{d}\mathbf{k}\,\mathrm{d}\mathbf{x}.$$

It is straight-forward to verify that $\mathcal{H}$ is a Casimir of the metric bracket. Any smooth function $f : \mathbb{R} \to \mathbb{R}$ defines a Casimir for the Poisson bracket via

$$\mathcal{C}[\rho](t) = \int_{\mathbb{R}^3}\int_{\mathbb{R}^3} f(\rho(\mathbf{x}, \mathbf{k}, t))\,\mathrm{d}\mathbf{k}\,\mathrm{d}\mathbf{x}.$$

We define an entropy functional $\mathcal{S}$ by the choice $f(\rho) = \rho^2/2$. The dynamics embodied in (1) can then be recovered from the abstract evolution (3) by considering functionals of the form

$$\mathcal{F}[\rho](t) = \int_{\mathbb{R}^3}\int_{\mathbb{R}^3} \psi(\mathbf{x}, \mathbf{k})\,\rho(\mathbf{x}, \mathbf{k}, t)\,\mathrm{d}\mathbf{k}\,\mathrm{d}\mathbf{x} \quad \text{for arbitrary test functions } \psi.$$

As a next step, the metriplectic formalism allows to systematically discretise the radiative transfer equation such that the first two laws of thermodynamics hold also for the discrete formulation, cf. [6].

References

[1] S. R. Arridge, J. C. Schotland. Optical tomography: forward and inverse problems. *Inverse Probl.* 25(12):123010, 2009.
[2] S. Chandrasekhar. *Radiative Transfer*. Dover, 1960.
[3] P. Gérard, P. A. Markowich, N. J. Mauser, F. Poupaud. Homogenization limits and Wigner transforms. *Communications on pure and applied mathematics*, 50 (4):323-379, 1998.
[4] M. Grmela. Bracket formulation of dissipative fluid mechanics equations. *Physics Letters A*, 102 (8):355–358, 1984.
[5] A. N. Kaufman. Dissipative Hamiltonian systems: A unifying principle. *Physics Letters A*, 100 (8):419–422, 1984.
[6] M. Kraus and E. Hirvijoki. Metriplectic integrators for the Landau collision operator. *Phys. Of Plasmas* 24(10):102311, 2017.
[7] M. I. Mishchenko. Poynting–stokes tensor and radiative transfer in discrete random media: the microphysical paradigm. *Optics Express*, 18(19): 19770, 2010.
[8] P. J. Morrison. A paradigm for joined Hamiltonian and dissipative systems. *Physica D: Nonlinear Phenomena*, 18:410–419, 1986.
[9] L. Ryzhik, G. Papanicolaou, and J. B. Keller. Transport equations for elastic and other waves in random media. *Wave Motion*, 24:327–370, 1996.
[10] H. Sato and M. C. Fehler. Seismic Wave Propagation and Scattering in the Heterogeneous Earth, Springer-Verlag, Berlin, 1998.

Conforming finite element divdiv complexes and the application for the linearized Einstein-Bianchi system

Rui Ma

(joint work with Jun Hu, Yizhou Liang)

This talk presents the first family of conforming finite element divdiv complexes on tetrahedral grids in three dimensions. In these complexes, finite element spaces of $H(\mathrm{divdiv}, \Omega; \mathbb{S})$ are from a current preprint [Chen and Huang, arXiv: 2007.12399, 2020] while finite element spaces of both $H(\mathrm{symcurl}, \Omega; \mathbb{T})$ and $H^1(\Omega; \mathbb{R}^3)$ are newly constructed here. It is proved that these finite element complexes are exact. As a result, they can be used to discretize the linearized Einstein-Bianchi system within the dual formulation.

References

[1] L. Chen and X. Huang, *Finite elements for divdiv-conforming symmetric tensors in three dimensions*, arXiv:2007.12399, (2020).
[2] J. Hu, Y. Liang and R. Ma, *Conforming finite element DIVDIV complexes and the application for the linearized Einstein-Bianchi system*, arXiv:2103.00088, (2021).
[3] V. Quenneville-Bélair, *A new approach to finite element simulation of general relativity*, PhD thesis, University of Minnesota, Minneapolis, 2015.
[4] D. Pauly and W. Zulehner, *The divdiv-complex and applications to biharmonic equations*, Applicable Analysis **99** (2020), 1579–1630.

Introduction to port-Hamiltonian systems

Hans Zwart

Starting with the standard Hamiltonian system given as

$$\begin{bmatrix}\dot{q}\\ \dot{p}\end{bmatrix} = \begin{bmatrix}0 & I\\ -I & 0\end{bmatrix} \frac{\partial H}{\partial(q,p)}(q,p),$$

we show that there are two generalisations possible. Namely, replacing the matrix $\left[\begin{smallmatrix}0 & I\\ -I & 0\end{smallmatrix}\right]$ by a general skew-symmetric matrix J, and secondly by allowing variables which model the connection with the environment, i.e., the ports. This led to the concept of a *Dirac structure*.

Let $\mathcal{E}$ and $\mathcal{F}$ be two linear spaces (*effort* and *flow* space, respectively) which are dual to each other with duality product $\langle f \mid e\rangle$. On the product space $\mathcal{B} := \mathcal{F} \times \mathcal{E}$ we define the symmetric bilinear form

$$\left\langle \begin{bmatrix}f_1\\ e_1\end{bmatrix}, \begin{bmatrix}f_2\\ e_2\end{bmatrix} \right\rangle_B = \langle f_2 \mid e_1\rangle + \langle f_1 \mid e_2\rangle.$$

The linear subspace $\mathcal{D} \subset \mathcal{B}$ is a *Dirac structure* if

$$\mathcal{D} = \mathcal{D}^{\perp},$$

where the $\perp$ is taken with respect to the bilinear form $\langle \cdot, \cdot \rangle_B$.

It is easy to see that for any Dirac structure there holds that $\langle f, e\rangle_B = 0$ for $\left[\begin{smallmatrix}f_1\\ e_1\end{smallmatrix}\right] \in \mathcal{D}$.

These Dirac structures might have external ports which can be coupled. A typical element of $\mathcal{D}_I$ looks like (f_1, f_c, e_1, e_c) and a typical element of $\mathcal{D}_{II}$ looks like $(f_2, \tilde{f}_c, e_2, \tilde{e}_c)$. Then

$$\begin{aligned}\mathcal{D}_{I \circ II} := \{ f_2, f_1, e_2, e_1) \in \mathcal{F}_2 \times \mathcal{F}_1 \times \mathcal{E}_2 \times \mathcal{E}_1 \mid \\ \text{there exist } f_c \in \mathcal{F}_c \text{ and } e_c \in \mathcal{E}_c \text{ such that} \\ (f_1, f_c, e_1, e_c) \in \mathcal{D}_I \text{ and } (f_2, f_c, e_2, -e_c) \in \mathcal{D}_{II}\}.\end{aligned}$$

is a Dirac structure.

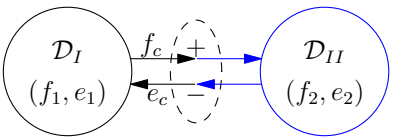

Figure 1. Coupling of two Dirac structures

There is a rich literature dealing with Dirac structures and port-Hamiltonian systems on finite-dimensional effort/flow spaces, see e.g. [1, 4, 5].

For infinite-dimensional flow and effort spaces, the theory can be extended. The start was given in [6]. The systems become partial differential equations, and thus the effort and flow spaces become function spaces. The J matrix is replaced by a (formally) skew-symmetric operator. For J given by $J = P_1 \frac{\partial}{\partial \zeta} + P_0$ the following

defines a Dirac structure on $\mathcal{F} = \mathcal{E} = L^2(a,b;\mathbb{R}^n) \oplus \mathbb{R}^n$ with the standard inner product, see e.g. [3, 7]

$$\mathcal{D} = \{(f, f_\partial, e, e_\partial) \mid e \in H^1(a,b;\mathbb{R}^n), f \in L^2(a,b;\mathbb{R}^n), f_\partial, e_\partial \in \mathbb{R}^n, \\ f = Je \text{ and } \begin{pmatrix} f_\partial \\ e_\partial \end{pmatrix} = \frac{1}{\sqrt{2}} \begin{pmatrix} P_1 & -P_1 \\ I & I \end{pmatrix} \begin{pmatrix} e(b) \\ e(a) \end{pmatrix} \Big\}.$$

P.d.e.'s associated to this Dirac structure have nice analytic and systems theoretic properties, see e.g [2, 3, 7]. The variables f_∂ and e_∂ may represent control and observations at the boundary of the spatial domain, but they can also be used to as interconnection variables. For instance when the differential operator J is replaced by a skew-symmetric matrix, as happens in numerical approximation of the p.d.e., the approximate Dirac structure only represents a small part of the total p.d.e.. By using many copies of this Dirac structure, and connecting them via the variables f_∂ and e_∂, see Figure 2, a numerical approximation of the total p.d.e. is constructed while maintaining the Hamiltonian structure.

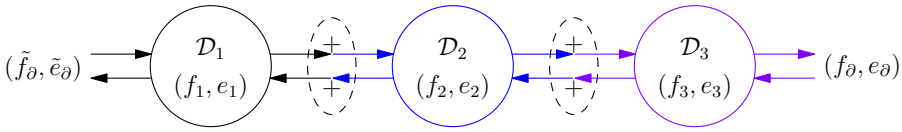

FIGURE 2. Coupling of Dirac structures via boundary effort and flow

REFERENCES

[1] V. Duindam, A. Macchelli, S. Stramigioli, and H. Bruyninckx, Eds., *Modeling and Control of Complex Physical Systems - The Port-Hamiltonian Approach*. Berlin, Germany: Springer-Verlag, 2009.

[2] B. Jacob and H.J. Zwart. *Linear Port-Hamiltonian Systems on Infinite-Dimensional Spaces*. Basel: Birkhäuser, 2012.

[3] Y. Le Gorrec, H. Zwart, and B. Maschke. Dirac structures and boundary control systems associated with skew-symmetric differential operators. *SIAM Journal on Control and Optimization*, 44(5):1864–1892, 2005.

[4] A.J. van der Schaft, Port-Hamiltonian systems: an introductory survey, International Congress of Mathematics, 2006.

[5] A.J. van der Schaft and D. Jeltsema. Port-Hamiltonian Systems Theory: An Introductory Overview, FnT in Systems and Control, Vol. 1, No. 2-3 (2014) 173–378.

[6] A. J. van der Schaft and B. M. Maschke. Hamiltonian formulation of distributed-parameter systems with boundary energy flow. *Jour. of Geometry and Physics*, 42:166–194, 2002.

[7] J.A. Villegas. *A port-Hamiltonian Approach to Distributed Parameter Systems*. PhD thesis, Universiteit Twente, 2007.

Adaptive boundary control for PDEs by Funnel Control

Felix L. Schwenninger
(joint work with Marc Puche, Timo Reis)

Boundary control for evolution equations is a classical topic in the control of infinite-dimensional systems and naturally appears when measurements and control inputs enter via interfaces of the spatial domain. Subtleties usually arise when identifying the respective boundary spaces. In the case of feedback control, this results in an implicit equation for which wellposedness needs to be investigated. Here, we consider an abstract class of linear boundary control systems of the form

$$\begin{aligned} \dot{z}(t) &= \mathfrak{A}z(t), \qquad z(0) = z_0, \\ \mathfrak{B}z(t) &= u(t), \\ \mathfrak{C}z(t) &= y(t), \qquad t > 0, \end{aligned}$$

with unbounded linear operators $\mathfrak{A}, \mathfrak{B}, \mathfrak{C}$, representing the *open loop* with input u, output y and state variable z. The nonlinear feedback law

$$u = \mathcal{F}(y)$$

is designed such that y, in the resulting implicit system, is arbitrarily close to a pre-given reference trajectory y_{ref}. This is achieved by penalizing the error between y and y_{ref} through a higher control gain. The considered approach follows the philosophy of *funnel control*, a well-studied methodology for nonlinear ODE systems [3], which recently has attracted growing interest in the context of infinite-dimensional system theory [1, 2, 5]. The structural assumptions on the system class allows for classical methods from nonlinear semigroup theory for showing wellposedness and feasibility of the control objective. These conditions involve dissipativity of the boundary control system and existence of solutions to certain associated elliptic problems. In particular, these abstract assumptions allow for hyperbolic as well as parabolic examples. Furthermore, the techniques also suggest extensions to nonlinear and non-autonomous open-loop systems.

This talk is based on the recent joint work [4] with Marc Puche and Timo Reis.

References

[1] T. Berger, T. Breiten, M. Puche and T. Reis. *Funnel control for the monodomain equations with the Fitz Hugh-Nagumo model*, *J. Diff. Eqns.* **286** (2021), 164–214.

[2] T. Berger, M. Puche and F.L. Schwenninger, *Funnel control in the presence of infinite-dimensional internal dynamics*, *Systems Control Lett.*, **32** (2020), 104678.

[3] A. Ilchmann, E. P. Ryan and C. J. Sangwin. *Tracking with prescribed transient behaviour*, *ESAIM: Control, Optimisation and Calculus of Variations*, **7** (2002), 471–493.

[4] M. Puche, T. Reis and F.L. Schwenninger, *Funnel control for boundary control systems*, *Evol. Eq. Control Th., to appear, DOI: 10.3934/eect.2020079* (2021).

[5] T. Reis and T. Selig, *Funnel control for the boundary controlled heat equation*, *SIAM J. Control Optim.*, **53**(1) (2015), 547–574.

Stress Approximation and Stress Equilibration in (Electro-)Elasticity

Gerhard Starke

(joint work with Fleurianne Bertrand, Marcel Moldenhauer)

Our point of departure is the approximation $\mathbf{u}_h$ satisfying the discretized optimality condition

$$(\partial_{\mathbf{F}}\psi(\mathbf{B}(\mathbf{u}_h), \nabla \mathbf{v}_h)_{L^2(\Omega)} = (\mathbf{f}, \mathbf{v}_h)_{L^2(\Omega)} + \langle \mathbf{t}, \mathbf{v}_h \rangle_\Gamma \text{ for all } \mathbf{v_h} \in \mathbf{V}_h$$

in some finite element space $\mathbf{V}_h$. Here, $\psi(\mathbf{B})$ is some free energy function, $\mathbf{B} = \mathbf{F}\mathbf{F}^T$ denotes the left Cauchy-Green strain tensor and $\mathbf{F} = \mathbf{F}(\mathbf{u}) = \mathbf{I} + \nabla \mathbf{u}$ the deformation gradient, while $\mathbf{f}$ and $\mathbf{t}$ are prescribe volume and traction forces, respectively. For the Piola-Kirchhoff stress tensor $\mathbf{S} = \partial_{\mathbf{F}}\psi(\mathbf{B}(\mathbf{u}))$, an approximation $\mathbf{S}_h^R$ satisfying exactly the equilibrium of momentum $\operatorname{div} \mathbf{S}_h^R + \mathbf{f} = \mathbf{0}$ is of interest. Such an equilibrated stress reconstruction may be computed as a correction $\mathbf{S}_h^R = \partial_{\mathbf{F}}\psi(\mathbf{B}(\mathbf{u}_h)) + \mathbf{S}_h^\Delta$ which may be localized to vertex patches using the corresponding partition of unity. The construction in [1], based upon our earlier investigation in [2], uses broken Raviart-Thomas spaces of next-to-lowest order and enforces the symmetry condition for the associated Cauchy stress $\mathbf{S}_h^\Delta \mathbf{F}(\mathbf{u}_h)^T$ weakly in the spirit of the stress finite element approach suggested in [3].

The structure of the local problems is studied in detail in [1] leading to the result that, for interior vertex patches, the null space of the adjoint operator (leading to linearly dependent constraints) is given by rigid body modes on the deformed configuration $(\mathbf{id} + \mathbf{u}_h)(\Omega)$.

The mathematical modelling of electro-elasticity is of interest, for example, in the context of dielectric elastomer actuators. Due to the large size of the associated strains, nonlinear elasticity formulations need to be used. The electromagnetic phenomena are described via the so-called electrostatic Maxwell stress

$$\mathbf{S}_m = \mathbf{D} \otimes \mathbf{E} - \frac{1}{2}\varepsilon(\mathbf{E} \cdot \mathbf{E})\, \mathbf{I}\,,$$

where $\operatorname{curl} \mathbf{E} = \mathbf{0}$ holds for the electric field E and the electric displacement D satisfies $\operatorname{div} \mathbf{D} = \rho$, the density of free charges. The coupling to the hyperelastic material model occurs in the modified equilibrium equation

$$\operatorname{div}(\mathbf{S} + \mathbf{S}_m) + \mathbf{f} = \mathbf{0}$$

(cf. [4]).

References

[1] F. Bertrand, M. Moldenhauer, G. Starke, *Weakly symmetric stress equilibration for hyperelastic material models*, GAMM-Mitteilungen **43** (2020), e202000007.

[2] F. Bertrand, M. Moldenhauer, G. Starke, *Weakly symmetric stress equilibration and a posteriori error estimation for linear elasticity*, Numer. Methods Partial Differential Equations (2021), DOI:10.1002/num.22741.

[3] D. Boffi, F. Brezzi, M. Fortin, *Reduced symmetry elements in linear elasticity*, Commun. Pure Appl. Anal. **8** (2009), 95–121.

[4] L. Dorfmann, R. W. Ogden, *Nonlinear electroelasticity: material properties, continuum theory and applications*, Proc. R. Soc. A **473** (2017), 20170311.

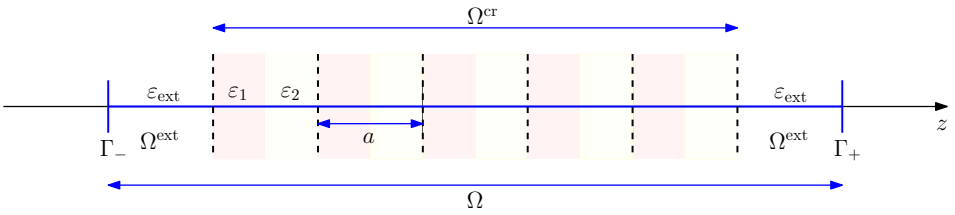

FIGURE 1. Bragg stack. Each unit cell has length a and consists of two materials material with permittivities ε_1 and ε_2. This unit cell is periodically repeated several times to create the photonic crystal Ω^{cr}. This structure is surrounded by a homogeneous medium with permittivity $\varepsilon_{\mathrm{ext}}$. The infinite computational domain is truncated to the interval $\Omega = \Omega^{\mathrm{cr}} \cup \Omega^{\mathrm{ext}} = [\Gamma_-, \Gamma_+]$.

Multiscale FEM for light propagation in realistic photonic crystals

MAREK KOZON

(joint work with Lars J. Corbijn van Willenswaard, Willem L. Vos, Matthias Schlottbom, Jacobus J. W. van der Vegt)

Photonic crystals are media with periodic spatial dependence of electric permittivity ε. This periodicity is responsible for highly nontrivial optical response to light passing through such a crystal. If properly designed, photonic crystals allow for manipulation of light, which leads to various applications [1], such as in optical components, solar cells, lasers, or quantum computing.

Due to the inherent complexity of these materials, numerical computations are a crucial tool in order to understand their interaction with light. Nevertheless, full three-dimensional (3D) models of light propagation through photonic crystals turn out to be extremely computationally demanding. This is mostly due to the multiscale character of the problem: The *micro-scale* is here represented by the unit-cell, *i.e.*, the smallest periodically repeated domain. On this domain, the electro-magnetic-field profile needs to be resolved with a sufficiently high accuracy. On the other hand, realistic photonic crystals used in the state-of-the-art experiments contain between 10^3 and 10^4 unit cells. This represents the *macro-scale*, over which the resolution needs to be maintained. In order to alleviate this issue, we aim to develop a *size-robust method*, *i.e.*, a method with computational complexity independent of the size of the crystal.

We illustrate our method on a one-dimensional photonic crystal, also known as a Bragg stack. The schematic of our computational domain is illustrated in Fig. 1. To compute the electromagnetic field profile in Ω, we solve the Helmholtz equation

$$\partial_z^2 u(z) + \left(\frac{\omega}{c}\right)^2 \varepsilon(z) u(z) = 0, \qquad \text{for all } z \in \Omega, \tag{1}$$

where u is the electric field to be found, ω and c are the frequency and the speed of light, respectively. We employ the non-reflecting boundary conditions

$$\mp\partial_z u(\Gamma_\mp) - \mathrm{i}k_{\mathrm{ext}}u(\Gamma_\mp) = \mp\partial_z u^{\mathrm{inc}}(\Gamma_\mp) - \mathrm{i}k_{\mathrm{ext}}u^{\mathrm{inc}}(\Gamma_\mp), \tag{2}$$

where we assume an incident plane wave $u^{\mathrm{inc}}(z) = e^{\mathrm{i}k_{\mathrm{ext}}z}$ coming from the left. To solve (1), we employ Discontinuous Galerkin FEM in the Symmetric interior penalty framework [2]. By properly choosing the space V^{gfem} of our trial and test functions, we are able to achieve computational size robustness. In the following, we will motivate and describe our definition of this space.

In order to motivate our choice of V^{gfem}, let us briefly look at a so-called unit-cell problem. This corresponds to solving the Helmholtz equation (1) in a setting with no external medium, *i.e.*, we assume that the Bragg stack extends to the infinity and the whole structure is thus globally periodic. From Bloch's theorem [3], it follows that the solutions of the unit-cell problem have the form of so-called Bloch modes:

$$u^{\mathrm{Bloch}}(z) = u_{\mathrm{per}}(z)e^{\mathrm{i}kz}, \tag{3}$$

where $u_{\mathrm{per}}(z) = u_{\mathrm{per}}(z+a)$ has the same periodicity as the medium and k is the wave vector corresponding to ω.

Bloch modes are therefore solutions for an idealized infinite photonic crystal. Based on this, one can expect that, for a finite but large crystal, they will still approximate the true solution to a very good extent. Indeed, it has been proposed by Brandsmeier *et al.* [4, 5] that Bloch modes could be used to construct the FEM basis functions to solve the problem (1). In their work, they modulate the Bloch modes by Lagrange polynomials of degree p_{mac} to construct the multiscale basis functions within the crystal. Using the character of these multiscale functions, they have developed an *essentially* size robust quadrature, with computational complexity scaling as $\mathcal{O}(\log N_{\mathrm{cr}})$, with N_{cr} being the number of unit cells in the crystal. Nevertheless, in order to maintain continuity on the interfaces, they are forced to introduce overlap elements at the boundary of the crystal which contain both multiscale functions and pure Lagrange polynomials. It turns out that in order to achieve sufficient resolution in these overlap elements, the required value of p_{mac} grows very fast with the frequency ω.

Instead, we propose to construct the trial and test space V^{gfem} as follows (for illustration, see Fig. 2). In the external medium, we define a mesh with Lagrange basis functions of order p_{ext} discontinuously coupled over the element interfaces. Inside the crystal, we treat the whole crystal as one element, using n_{Bloch} Bloch modes as basis functions. In the language of functional spaces, we define our trial and test space as

$$V^{\mathrm{gfem}}(\Omega) = V^{\mathrm{Bloch}}(\Omega^{\mathrm{cr}}) + \mathbb{P}^{p_{\mathrm{ext}}}(\Omega^{\mathrm{ext}}), \tag{4}$$

where V^{Bloch} is the space of n_{Bloch} Bloch modes and $\mathbb{P}^{p_{\mathrm{ext}}}$ is the standard broken polynomial space.

Because our basis functions within the crystal are pure, unmodulated, Bloch modes, the quadrature of [5] becomes truly size robust, *i.e.*, independent of the

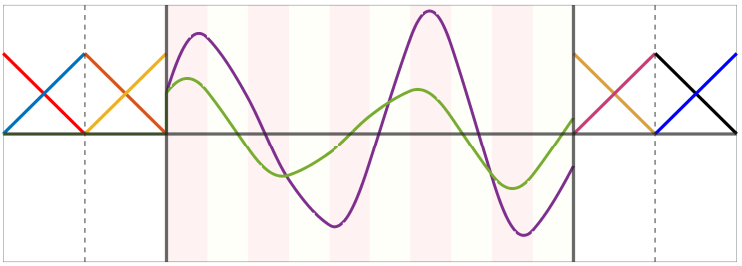

FIGURE 2. Schematic of the V^{gfem} basis functions of our method. Each color represents a separate function.

crystal size N_{cr}. Moreover, our method does not require overlap elements at the crystal boundary, which means that the accuracy decrease w.r.t. the frequency ω is significantly alleviated.

We finalize by outlining our method in four simple steps:
Micro-scale:

(1) Compute the Bloch modes by solving the unit-cell problem.

Macro-scale:

(2) Use Bloch modes as DG basis functions inside the crystal.
(3) Assemble the stiffness matrix using the size-robust quadrature.
(4) Solve the resulting linear system of equations.

Next step in out research is to develop a proper theoretical analysis of convergence of our method. Afterwards, we aim for implementation in two and three dimensional problems, also obtaining physically relevant results.

REFERENCES

[1] S. Noda *Two decades of progress for photonic crystals: from the realization of complete 3D crystals to the state of the art for society 5.0*, Proc. SPIE 10927 (2019)
[2] D. A. Di Pietro, A. Ern, *Mathematical Aspects of Discontinuous Galerkin Methods*, Springer (2012)
[3] J. A. Joannopoulos, S. G. Johnson, J. N. Winn, R. D. Meade, *Photonic crystals*, Princeton University Press (2008)
[4] H. Brandsmeier, K. Schmidt, Ch. Schwab, *A multiscale* hp*-FEM for 2D photonic crystal bands*, J. Comput. Phys. **230** (2011), 349–374.
[5] H. Brandsmeier, *Standard and Generalized hp-Finite Element Discretizations for Periodic Structures*, PhD Thesis, ETH Zürich (2013).

Reporter: Maurice Hensel

Participants

Prof. Dr. Fleurianne Bertrand
Department of Mathematics
and Computer Science
University of Twente
P.O. Box 217
7500 AE Enschede
NETHERLANDS

Mr. Lars Corbijn van Willenswaard
Systems, Analysis and Computational
Sciences (SACS),
University of Twente
P.O. Box Postbus 217
7500 AE Enschede
NETHERLANDS

Dr. Elena Giammatteo
Department of Mathematics
and Computer Science
University of Twente
Postbus 217
7500 AE Enschede
NETHERLANDS

Maurice Hensel
Fakultät für Mathematik
Universität Duisburg-Essen
Thea-Leymann-Straße 9
45127 Essen
GERMANY

Martin Hutzenthaler
Fakultät für Mathematik
Universität Duisburg-Essen
Mathematikcarrée
Thea-Leymann-Straße 9
45127 Essen
GERMANY

Mr. Marek Kozon
Department of Mathematics
and Computer Science
University of Twente
Postbus 217
7500 AE Enschede
NETHERLANDS

Dr. Agnes Lamacz-Keymling
Fakultät für Mathematik
Universität Duisburg-Essen
Thea-Leymann-Strasse 9
45127 Essen
GERMANY

Kaifung Liu
Department of Applied Mathematics
University of Twente
P.O.Box 217
7500 AE Enschede
NETHERLANDS

Dr. Rui Ma
Fakultät für Mathematik
Universität Duisburg-Essen
Thea-Leymann-Straße 9
D-45127 Essen
GERMANY

Dr. Carlos Pérez Arancibia
Facultad de Matematicas
Pontificia Universidad Católica de Chile
Av Vicuña Mackenna 4860, Macul
0 Santiago 0
CHILE

Emilie Pirch
Institut für Mathematik
Humboldt-Universität Berlin
Rudower Chaussee 25
12489 Berlin
GERMANY

Prof. Dr. Matthias Schlottbom
Department of Mathematics
and Computer Science
University of Twente
Postbus 217
7500 AE Enschede
NETHERLANDS

Henrik Schneider
Institut für Mathematik
Humboldt-Universität zu Berlin
Unter den Linden 6
10117 Berlin
GERMANY

Dr. Felix Schwenninger
Department of Applied Mathematics
University of Twente
P.O. Box 217
7500 AE Enschede
NETHERLANDS

Prof. Dr. Gerhard Starke
Fakultät für Mathematik
Universität Duisburg-Essen
Thea-Leymann-Strasse 9
45127 Essen
GERMANY

Prof. Dr.Ir. Jaap J.W. van der Vegt
Department of Applied Mathematics
Faculty of Electrical Engineering,
Mathematics and Computer Science
University of Twente
P.O. Box 217
7500 AE Enschede
NETHERLANDS

Prof. Dr. Irwin Yousept
Fakultät für Mathematik
Universität Duisburg-Essen
Thea-Leymann-Straße 9
45127 Essen
GERMANY

Prof. Dr. Hans J. Zwart
Department of Applied Mathematics
University of Twente
P.O. Box 217
7500 AE Enschede
NETHERLANDS